



GROUNDWATER FLOW THROUGH A
CONSTRUCTED TREATMENT WETLAND

THESIS

Jack A. Blalock, Captain, USAF

AFIT/GEE/ENV/03-01

DEPARTMENT OF THE AIR FORCE
AIR UNIVERSITY
AIR FORCE INSTITUTE OF TECHNOLOGY

Wright-Patterson Air Force Base, Ohio

APPROVED FOR PUBLIC RELEASE; DISTRIBUTION UNLIMITED

The views expressed in this thesis are those of the author and do not reflect the official policy or position of the United States Air Force, Department of Defense, or the U.S. Government.

AFIT/GEE/ENV/03-01

GROUNDWATER FLOW THROUGH A CONSTRUCTED TREATMENT WETLAND

THESIS

Presented to the Faculty

Department of Systems and Engineering Management

Graduate School of Engineering and Management

Air Force Institute of Technology

Air University

Air Education and Training Command

In Partial Fulfillment of the Requirements for the

Degree of Master of Science in Engineering and
Environmental Management

Jack A. Blalock, B.S.

Captain, USAF

March 2003

APPROVED FOR PUBLIC RELEASE; DISTRIBUTION UNLIMITED.

AFIT/GEE/ENV/03-01

GROUNDWATER FLOW THROUGH A CONSTRUCTED TREATMENT WETLAND

Jack A. Blalock, B.S.
Captain, USAF

Approved:

//Signed//

Dr. Michael L. Shelley (Chairman)

27 Feb 03

date

//Signed//

Dr. Mark N. Goltz (Member)

27 Feb 03

date

//Signed//

Dr. Junqi, Huang (Member)

27 Feb 03

date

Acknowledgements

I would like to thank my thesis advisor and committee chairman, Dr. Michael Shelley, for the chance to learn about the unique field of wetlands. You were always flexible and patient with the many obstacles throughout the study, always providing a new direction when needed.

I would also like to thank my other committee members: Dr. Mark Goltz, for providing expert technical support and turning my words into professional documentation, and Dr. Junqi Huang, for giving precise numerical modeling support; without your help, this thesis would be found lacking.

I must also thank my wife and son for their endurance for the many hours I spent with the computer instead of them.

Last, I must repeat what my predecessor, Maj Andrew C. Entingh, USMC, said in his acknowledgement, "I thank God for the aptitude to tackle graduate level studies and the opportunity to study a very small but intricate piece of His awesome creation. The whole earth proclaims your glory!" I could not have said it better myself.

Jack A. Blalock

Table of Contents

	page
Acknowledgements	iv
Table of Contents	v
List of Figures	vii
List of Tables	ix
I. Introduction	1-1
Background	1-1
Treatment Wetland Construction	1-4
Problem Statement	1-7
Research Questions	1-8
Scope and Limitations	1-8
II. Literature Review	2-1
Wetlands	2-1
Groundwater Flow	2-6
Main Equations of Flow	2-15
Residence-Time Distribution Function	2-16
Mapping Groundwater Flow	2-20
III. Methodology	3-1
Overview	3-1
Sampling Grid	3-1
Piezometer Installation	3-3
Piezometer Measurements	3-7
Groundwater and Soil Parameters	3-9
Numerical Model	3-17
Residence Time Distribution Function (RTDF)	3-22
IV. Results	4-1
Piezometer Installation	4-1
Piezometer Measurements	4-2
Explanation for Unexpected Head Measurements	4-3
Parameter Estimation	4-7
Numerical Model	4-8
Residence Time Distribution Function (RTDF)	4-20

	page
V. Conclusions and Recommendations for Further Study	5-1
Study Strengths	5-2
Study Weaknesses	5-3
Recommendations for Further Study	5-4
Appendix A: Piezometer Data	5.1-1
Appendix B: Porosity Data	5.2-1
Appendix C: Slug Test Data	5.3-1
Appendix D: Equipotential Head Contour Plots	5.4-1
Appendix E: Cross-Sections of the Wetland Model	5.5-1
Appendix F: Location Data of Particles Through Wetland	5.6-1
Appendix G: Residence Time Distribution Function Data	5.7-1
Bibliography	5.7-1
Vita	5.7-1

List of Figures

	page
Figure 1-1. Concept Design of the Wright-Patterson Air Force Base Wetland Treatment Cells	1-5
Figure 2-1. Experimental Apparatus for Illustration of Darcy's Law	2-7
Figure 2-2. Sample Flow Net (Entingh, 2001:2-30)	2-9
Figure 2-3. Four Combinations of Heterogeneity and Anisotropy, Adapted from Freeze and Cherry, 1979	2-14
Figure 2-4. RTDF Example	2-18
Figure 2-5. Cumulative RTDF Example	2-20
Figure 3-1. Piezometer Placements	3-2
Figure 3-2. Driving Piezometers with a Slide Hammer	3-4
Figure 3-3. Piezometer Placement Cross-section	3-5
Figure 3-4. Bentonite Placement Diagram	3-6
Figure 3-5. Locations of Well Nests	3-13
Figure 3-6. Field Response of a Slug Test	3-17
Figure 3-7. Injection Wells—Top View	3-20
Figure 3-8. Particle Locations in Three Adjacent Injection Cells	3-23
Figure 4-1. Areas of White Showing Upward Flow	4-5
Figure 4-2. Actual Piezometer Placement Cross-section	4-6
Figure 4-3. Hydraulic Conductivity Example	4-9
Figure 4-4. Extraction Wells Viewed from Top	4-11
Figure 4-5. Calculated Vs. Observed Head	4-12

	page
Figure 4-6. Contours of Equipotential Head of Layer 1 From the Top	4-14
Figure 4-7. Lengthwise Elevation Profile Along the Mid-section of the Wetland Showing Equipotential Head Contours	4-14
Figure 4-8. Widthwise Elevation Profile Along the Midsection of the Wetland Showing Equipotential Head Contours	4-14
Figure 4-9. Equipotential Head Surface Plot for the Top Layer	4-15
Figure 4-10. Elevation View Showing Flow Directions	4-16
Figure 4-11. View of Paths of Selected Molecules	4-18
Figure 4-12. Elevation Profile of Molecule Paths	4-19
Figure 4-13. Width Elevation Profile of Molecule Paths	4-19
Figure 4-14. Cumulative RTDF	4-20
Figure 4-15. RTDF	4-21

List of Tables

	page
Table 1-1. Composition of the Soil Layers	1-6
Table 4-1. Porosity and Specific Yield Data	4-7
Table 4-2. Hydraulic Conductivities (ft/s)	4-8
Table 4-3. Model Hydraulic Conductivities	4-9
Table 4-4. Residence Times	4-19

Abstract

This study is an analysis of the flow of water through a constructed treatment wetland at Wright-Patterson AFB, OH. The purpose of the treatment wetland is to biodegrade perchloroethylene, which is present in the groundwater as a contaminant. Contaminated water enters the bottom of the wetland and flows upward, exiting the wetland from a weir at one end. The wetland is designed for water to move vertically through the soil layers composing the wetland. The main purpose of this study is to characterize the water flow through the different layers of soil in the wetland.

In this study, hydraulic parameters are measured and then used to build a numerical model of the wetland system. The model is then run to simulate flow through the wetland, in order to develop a residence time distribution function (RTDF). The RTDF tells us what fraction of water (and contaminant) molecules can be expected to be in the wetland for a given time. This information is needed to predict the overall extent of contaminant degradation within the system. It was determined that for the fraction of influent water that ultimately flowed out the weir, the mean residence time was 1.6 days.

GROUNDWATER FLOW THROUGH A CONSTRUCTED TREATMENT WETLAND

I. Introduction

The purpose of this study is to characterize the groundwater flow through a constructed treatment wetland. This study is a comparison and continuation of a previous thesis by Major Andrew C. Entingh, USMC, using the same techniques to characterize the water flow, but with different wetland soil conditions. By characterizing groundwater flow through a constructed treatment wetland, one can visualize the flow paths of water through various types of soil. With better flow path information, an intuition for the residence time of molecules in the wetland is obtained, thus providing a better understanding of the extent of reactions that may occur which affect the fate of contaminant in the wetland "reactor."

Background

The 20th century has seen a tremendous increase in technology, which brought about a greater reliance on chemicals. Unfortunately, very little was known about the damage that these chemicals could cause to the environment

if released. This lack of knowledge resulted in a rise in groundwater pollution. In the case where groundwater pollution has already occurred, the United States Environmental Protection Agency (EPA) requires cleanup of these areas under the Comprehensive Environmental Response, Compensation, and Liability Act (CERCLA), commonly known as Superfund.

The Superfund Program, which resulted from the enactment of CERCLA, has focused government and private industry funds and attention on the cleanup of hundreds of sites with contaminated groundwater. Many of these sites have come from previous poor management of chemicals. Over time these chemicals have been transported by flowing groundwater and are now appearing in drinking water wells. Since contamination originated from government practices at many of these sites, it is the responsibility of the government to restore the purity of the water at these sites. The Air Force alone has identified 2580 potentially contaminated sites. Although 1398 of these 2580 sites have been dealt with to date (either having been found not to pose a risk, or by remediation), the Air Force still spends around \$400 million per year cleaning sites.

A large number of the U.S. Air Force (USAF) contaminated sites have high levels of chlorinated ethenes

such as perchloroethylene (PCE), trichloroethene (TCE), various isomers of dichloroethene (DCE), and vinyl chloride (VC). Many of these contaminants are common industrial solvents, and are used in industries as varied as dry-cleaning and plastic production. Pollution at sites owned by the USAF often stems from previous poor management practices, such as allowing degreasing solvents to run off onto the ground.

The high cost of remediation has brought about a search for a less expensive method to accomplish the goal of decontamination. One possible solution is the process called natural attenuation. This method relies on natural processes, specifically microbial activity, to purify water. Microbial activity takes place in environments that are high in the elements essential for microbial growth. One area that contains many of these essential elements is wetlands. Current research reveals that wetlands could be ideal environments for the natural attenuation of contaminants through complete biodegradation. (Lorah & Olsen, 1999: 3811)

Wetlands are land areas in which saturated soil conditions and vegetation are maintained throughout the year due to the water table positioned at or above the ground (Reed et al., 1995). The saturated soil provides an

ideal environment for plants to flourish. As the plants flourish, many microorganisms can dwell in the area as well. A biologically rich environment is then provided which is optimal for degrading contaminants in water.

Treatment Wetland Construction

To utilize the wetland water purification technique, a wetland can be constructed. This construction is accomplished through the following steps. The first task is to determine the location of the contamination plume. This is accomplished through observation wells to determine the area of greatest contamination. The wetland should be constructed in an area where the contaminated water can be efficiently pumped into the wetland. Locating the wetland near the contaminated site can save cost and energy when choosing the correct pump size.

In order to evaluate the feasibility of using a wetland for remediation of contaminated groundwater, a wetland of two distinct cells was constructed at Wright-Patterson Air Force Base (WPAFB), OH, in the summer of 2000. The two cells were each 120 feet long, 60 feet wide, and 5 feet deep. A geomembrane liner was put in place to keep the contaminated water from going back into the ground. In the bottom of the pit, a pipe distribution

system was installed within a gravel layer that carries the contaminated groundwater into the wetland to distribute the flow evenly along the bottom through perforations in the pipe. Above the gravel layer, three more layers of soil were added. A weir installed at the end of the wetland allows for the outflow of water in a controlled manner.

Figure 1-1 represents the layout of a constructed wetland.

Note: drawing not to scale.

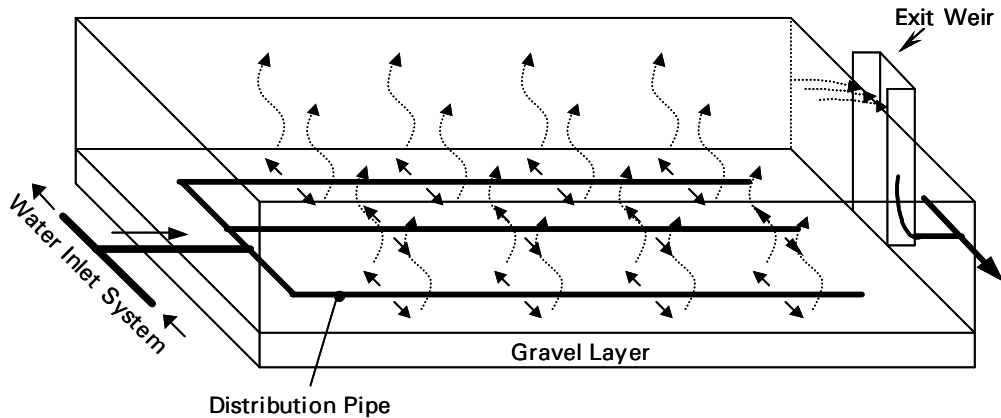


Figure 1-1 Concept Design of the Wright-Patterson Air Force Base Wetland Treatment Cells

The difference between the two different wetland cells developed at WPAFB is in the soils used. In both cells, hydric soil (soil from prior wetlands) was used in some layers. A summary of the soil used in the wetland cells is in Table 1-1.

Table 1-1 Composition of the Soil Layers

<u>Layer</u>	<u>Cell 1</u>	<u>Cell 2</u>
Top	Hydric Soil (likely root zone)	Hydric Soil (likely root zone)
Middle	Hydric Soil	Local, Iron-rich Fill
Bottom	Hydric Soil (organic matter added)	Hydric Soil

The difference in the bottom layers of the two cells is found in the organic matter added to cell one in the form of wood chips. This organic matter was added to help stimulate the anaerobic degradation of the PCE-contaminated water that entered the bottom of the cell.

The middle layers of the constructed cells differ in that local iron-rich soil was added to cell two. This soil was included to determine the effects of iron on vinyl chloride degradation. The iron provides oxidizing conditions under which it is hypothesized that VC is more readily degraded.

The top layers of the cells are the same. The hydric soil was taken from prior wetlands because it is a soil that greatly helps plants grow when completely saturated and is relatively high in organic content to support microbial activity.

The plants chosen for the wetland cells are plants that grow naturally in wetland environments with saturated soil. The plants vary between the cells, as well as within each cell. Plants are known to take chemicals into their

root systems and metabolize them, thereby helping the decontamination effort.

Information must be gathered regarding the process of contaminant degradation. Equally important, however, is the process by which water flows through the wetland. One relationship that is not well quantified is the relationship of the flow paths of water through a treatment wetland and the type of soil used for wetland construction. This relationship must be understood to help model contaminant degradation in constructed wetlands. This research, along with Major Entingh's research, should provide more information allowing us to describe flow in a constructed treatment wetland.

Problem Statement

A vertical-flow constructed treatment wetland is designed so that water flows vertically from the bottom to the top of the wetland, and then horizontally along the water surface to the outlet weir. Degradation occurs as the water flows vertically through the various wetland layers. In fact, such an idealized flow pattern is not seen. Flow is typically non-ideal, with the water molecules flowing through the wetland having large variations in residence times. These variations can affect

the efficiency of microbial degradation. A method to analyze the effect of varying residence times on the overall degradation efficiency of the wetland is needed. This analysis requires a study of flow patterns and residence times.

Research Questions

- (1) What paths do the water molecules take while flowing through each of the layers of the wetland?
- (2) Does the behavior of groundwater flow change with varying inlet flow rates?
- (3) What is the approximate residence time for groundwater molecules moving through the subsurface media, and how does this compare to the ideal residence time?
- (4) Can data from Major Entingh's thesis be used to build a similar residence time model for comparison of wetland cells?

Scope and Limitations

This research will characterize the groundwater flow through a constructed wetland with specific hydraulic parameters. Using data collected from the constructed wetland, the groundwater flow will be analyzed by use of a model that will provide a visual representation of the flow

dynamics. Similar data collected from a different constructed wetland will be modeled with the purpose of comparing residence times of the two wetlands. The comparison and model analysis should provide information that will be useful in understanding the operation and designing of constructed treatment wetlands.

II. Literature Review

This literature review provides a background to the methods used in characterizing the flow of groundwater through a constructed treatment wetland. The information provided herein should give the reader a clear understanding of the principal function of wetlands and the characteristics of a constructed treatment wetland. Also included is a detailed analysis of the principal factors that influence the paths of groundwater flowing through a wetland, the concepts behind use of a Residence Time Distribution Function to determine how long individual water molecules spend in the wetland, as well as information about current software available for helping to model flow through the wetland. Armed with this information, the reader will then be able to follow the methodology chosen to answer the questions posed in the first chapter.

Wetlands

How contaminated water flows through a wetland, and in particular, how long the contaminant molecules are in the wetland so that wetland remediation processes have time to operate, directly affects decontamination efficiency.

Knowledge of the characteristics of a wetland is imperative to understanding the dynamics of the flow. As mentioned before, wetlands are areas where water either covers the soil or is present at or near the surface of the soil all year, or for varying periods of time throughout the year. The degree of water saturation helps determine how the soil develops and the types of plant and animal communities living in and on the soil. Wetlands can support both aquatic and terrestrial species. The saturated conditions sustain the growth of microorganisms, adapted plants (hydrophytes), and the development of wetland (hydric) soils.

Microorganisms in Wetlands

Wetlands are ideal to support the growth of microscopic organisms (microorganisms). There is a constant supply of nutrients for growth. The two major microorganisms found in a wetland are bacteria and fungi.

The bacteria in a wetland serve as the primary instrument to affect pollutant degradation. The mechanism of degradation depends on the location of the bacteria. Many close to the surface are aerobic, while those that are deeper in the subsurface are anaerobic. This is useful because some contaminants, such as perchloroethylene, degrade only under anaerobic conditions, whereas others,

such as Vinyl Chloride, degrade most efficiently in aerobic conditions. The bacteria can ultimately transform contaminants to innocuous compounds, e.g. CO₂, H₂O, and NH₄. Another function of bacteria is the fixation of nitrogen from the atmosphere to the soil. Plants take up the nitrogen as an essential nutrient.

Fungi are in a separate kingdom than bacteria and represent yeasts, molds, and fleshy fungi. Like bacteria, there are different types of fungi that degrade contaminants in aerobic and anaerobic conditions. Yeasts, for example, can degrade organic matter to carbon dioxide and water through aerobic respiration or can live as facultative anaerobes by using organic compounds as terminal electron acceptors. (Knight & Kadlec, 1996:120)

Wetland Vegetation

There are currently over 600 plant species reported in treatment wetlands in the United States. The correct choice of plants for a constructed treatment wetland can greatly improve the degradation capabilities of the wetland. A variety of plants promote a large faunal diversity. (Knight, 1997:36)

Aquatic plants play many roles in a wetland, taking part in physical, chemical, and microbial processes. Physically, plants offer mechanical resistance to the flow

of water across the surface, which results in an increase in retention time (Gopal, 1999:29). The increased retention allows more time for biodegradation to occur.

Plants take part in chemical processes as they add oxygen to the anaerobic layers of the soil, thus helping in oxidation and precipitation of heavy metals on root surfaces. Submerged macrophytes (macroscopic plants) directly oxygenate water. Free-floating plants can completely eliminate oxygen in the water column to enhance reduction reactions. (Gopal, 1999:29)

Aquatic plants also play a role in microbial processes by providing a large surface for microbial growth. Plants remove nutrients from the water, which increases the degradation efficiency of microbes by helping control a buildup of nutrients. (Gopal, 1999:29)

Wetland Soil

The soil of a wetland is termed hydric soil. Hydric soils are defined as soils that formed under conditions of saturation, flooding, or ponding long enough during the growing season to develop anaerobic conditions in the upper part (Federal Register, July 13, 1994). The anaerobic conditions are a result of microbes living in saturated conditions depleting the oxygen.

Wetland soils fall into two categories: mineral soil and organic soil. Mineral soils have less than 12 to 20 percent organic carbon, whereas organic soils contain at least 12 to 20 percent carbon (Knight & Kadlec, 1996:63-64). The Hydric soil in the first and third layers of both wetland cells is organic. The soil placed in the second layer, on the other hand, is mineral.

The chemical properties of soil are related to the chemical reactivity of soil particles, which in turn is related to the surface area of the particles available for chemical reactions. Chemical reactivity is dependent on the surface electrical charge of the soil particles. Organic soils typically have a high soil charge. (Knight & Kadlec, 1996:69)

Biological properties of hydric soils are mostly due to microbial processes. Transformations of nitrogen, iron, sulfur, and carbon result from microbial processes. The microbial processes are greatly influenced by the concentration of reactants, in addition to the redox potential and pH of the soil. Other than microbial processes, other biological influences include algae, macrophytes, and animals within the wetland. (Knight & Kadlec, 1996:69)

Groundwater Flow

Water flowing through the ground has been studied for centuries. A clear understanding of what influences groundwater flow can be useful in many situations.

The primary parameter that is used to quantify the flow of water through a wetland is the linear, or pore velocity. This velocity depends on three major components: soil porosity, hydraulic conductivity, and hydraulic gradient. The latter two of these parameters are used in the Darcy equation to help determine velocity.

Darcy Equation

In 1856, Henry Darcy conducted experiments to determine what factors affect the velocity of water flowing through soil (See Freeze & Cherry, 1979; Domenico & Schwartz, 1998; and Masters, 1998, for example). His experiments were carried out using a cylinder with a known cross-sectional area as seen in Figure 2-1. The ratio of flow [L^3T^{-1}] to area [L^2] can be defined as the specific discharge, q [LT^{-1}].

$$q = \frac{Q}{A} \quad (1)$$

Darcy found that for a given two points in the cylinder, this specific discharge is directly proportional to the

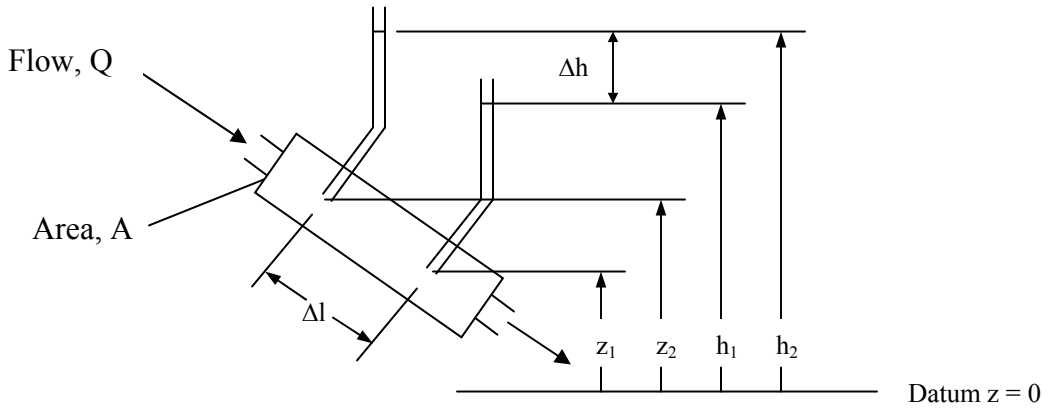


Figure 2-1 Experimental Apparatus for Illustration of Darcy's Law, from Freeze and Cherry, 1979.

difference in the hydraulic head measured at each of the two points ($h_2 - h_1$) (Freeze & Cherry, 1979: 16). The hydraulic head is a measure of the potential energy of the water (the sum of its elevation and pressure heads) and the kinetic energy of the water (its velocity head). Typically, though, the velocity head of groundwater is quite small relative to the pressure and elevation heads, and it is usually ignored. If this hydraulic head difference is held constant, then the specific discharge is inversely proportional to the distance along a flow line between the two points ($l_2 - l_1$). Using this relationship, Darcy's law can be written as

$$q = -K \cdot \frac{\Delta h}{\Delta l} \quad (2)$$

which can also be written in differential form as

$$q = -K \cdot \frac{dh}{dl} \quad (3)$$

The dh/dl in this equation is called the hydraulic gradient. The K is a proportionality constant known as the hydraulic conductivity. Each of these parameters will be discussed in more detail later. The sign convention is negative to indicate that water flows in the direction of decreasing hydraulic gradient.

The specific discharge defined in equation 3 can be applied back into equation 1 to provide an equation for the flow of water as

$$Q = -K \cdot \frac{dh}{dl} \cdot A \quad (4)$$

The specific discharge in equations 1 through 3 represents a velocity (the so-called Darcy velocity) that conceptually flows through the entire cross-sectional area, including the voids and solids of the soil. The actual velocity of the water molecules should only involve the voids because that is where the water actually flows. To compute an actual velocity (v), the cross-sectional area should be multiplied by porosity (n), so that equation 1 can be re-written

$$v = \frac{Q}{A \cdot n} \quad (5)$$

The velocity, v , is known as the average linear velocity or pore velocity. Note that

$$v = \frac{q}{n} \quad (6)$$

When equations 3 and 6 are combined, the average linear velocity can be written in terms of the hydraulic conductivity, hydraulic gradient, and porosity as follows

$$v = \frac{-K}{n} \cdot \frac{dh}{dl} \quad (7)$$

Once each of these three parameters is known for various points in a wetland, a flow net can be developed. Flow nets consist of flow lines and equipotential lines.

Equipotential lines are lines of constant hydraulic head.

Figure 2-2 illustrates a simple flow net.

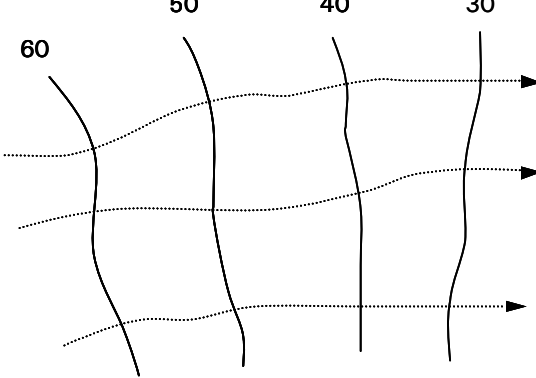


Figure 2-2 Sample Flow Net (Entingh, 2001:2-30)

In Figure 2-2, the solid lines are lines of equal potential, and the dashed lines are the flow lines.

Obtaining accurate estimates of the parameters in equation 7 can be challenging, therefore the next few

sections will discuss various techniques for their determination.

Porosity

Two parameters that may be used to quantify porosity are the total porosity and effective porosity. The total porosity of soil is a ratio of the volume of voids (openings) to the total volume of the material (Masters, 1998: 222). The equation defining total porosity (n) is as follows:

$$n = \frac{V_v}{V_T} \quad (8)$$

where V_v is the volume of the void space, and V_T is the total volume of the material. This porosity takes into account any and all void spaces in the porous material.

A common method for measuring total porosity is to first take a sample of saturated soil with a known volume. This volume is the total volume (V_T) discussed in equation 8. The next step is to weigh the sample, then bake the soil in an oven until completely dried, and then weigh it once more. This weight of the dried soil is termed the weight of the solids. The difference between the saturated weight and the dry weight is the weight of the water that was in the voids of the soil. The weight of the water divided by the density of water (1 kg/L) is the volume of

the water that was in the soil, or the volume of voids (V_v) in equation 8. Now that the two volumes are known, the ratio gives the total porosity.

When water flows through soil, some voids may not be connected to the flow paths of the water. Because of this, the term "effective porosity" is defined as the percentage of interconnected pore space (Domenico & Schwartz, 1998: 14). Depending on soil type, effective porosity may be considerably less than the total porosity.

Obtaining an accurate measure of effective porosity in the laboratory can be challenging. One method is simply to estimate the effective porosity by comparing the soil of interest with values of a similar soil in a table. Another method is to use the specific yield of the soil to estimate effective porosity.

The specific yield is the storage term for unconfined aquifers (Freeze & Cherry, 1979: 61). The equation for the specific yield is:

$$s_y = \frac{V_{wd}}{V_T} \quad (9)$$

where V_{wd} is the volume of water that drains from the soil due to gravity. The amount of water that drains from the soil can be determined in the laboratory. Once the initial saturated soil sample is weighed, it is placed in an

airtight container in order to prevent loss of water due to evaporation. The soil is then allowed to drain and weighed again. The difference in weights divided by the density of water is the volume of water that drained from the soil (V_{wd}). The ratio of the volume of the water drained to the original saturated soil volume is the specific yield.

Note that the method described above provides a laboratory estimate of specific yield, and it is strictly a function of the drained and total volumes of the subsurface material. As noted above, we are more interested in determining the effective porosity of the wetland material. Effective porosity, which is the percentage of interconnected pore space, is affected by the hydraulic gradient within a wetland. As the upward pressure is increased (increased flow), more pores within the soil participate in the flow. An increase in flow can also create more connections between pore spaces, leading to an increase in effective porosity.

Hydraulic Gradient

As noted earlier, the hydraulic gradient is the change in hydraulic head over some distance. The hydraulic head comes from the sum of the elevation, pressure, and velocity heads (where the velocity head is assumed to be zero due to very slow groundwater flow). The distance measured for the

hydraulic gradient must be in the direction of flow, whether horizontal, vertical, or any other direction. A more detailed explanation of the hydraulic gradient can be found in Entingh (2000) on pages 2-24 through 2-27.

Hydraulic Conductivity

The proportionality constant in the Darcy equation is called the hydraulic conductivity. It is a function of the fluid and the media (soil). For a highly viscous fluid, such as molasses, the hydraulic conductivity would be small, resulting in a small average linear velocity for a given hydraulic gradient. The hydraulic conductivity would be higher, however, for a less viscous fluid, such as water.

If water is the fluid being studied, as in this thesis, the hydraulic conductivity varies, depending on the media. It has higher values for sand or gravel and lower values for clay and most rock (Freeze & Cherry, 1979:16).

For a point chosen in the media, the hydraulic conductivity may not be the same in all directions. If conductivity is not the same in all directions, it is termed anisotropic. If, on the other hand, the hydraulic conductivity is the same in all directions, it is called isotropic. In the case where hydraulic conductivity varies

with location, it is termed heterogeneous, otherwise homogeneous.

For a graphic representation of hydraulic conductivity isotropy/anisotropy and homogeneity/heterogeneity, see Figure 2-3 (Freeze and Cherry, 1979).

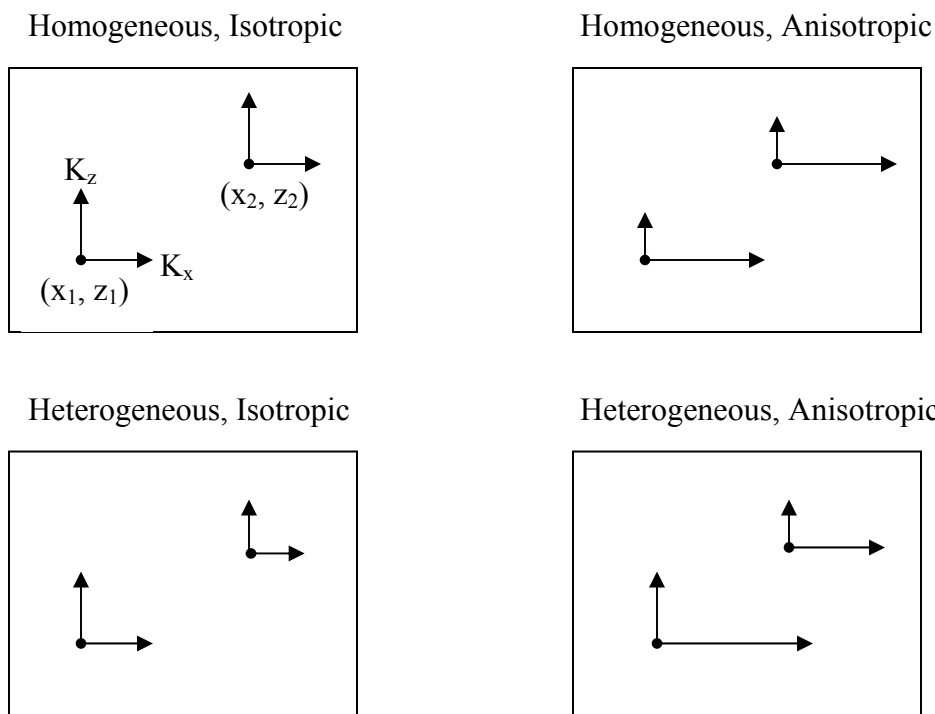


Figure 2-3 Four Combinations of Heterogeneity and Anisotropy, Adapted from Freeze and Cherry, 1979. K_x and K_z Represent Hydraulic Conductivity in the x- and z-directions, Respectively.

Note that equations 2 through 7, which are all versions of Darcy's Law, were derived assuming one-dimensional flow. When the hydraulic conductivity is not the same in all directions, we must account for this anisotropy in Darcy's Law. Freeze and Cherry (1979)

present the following three equations to characterize the Darcy equation under anisotropic conditions:

$$q_x = -K_x \frac{\partial h}{\partial x} \quad (10a)$$

$$q_y = -K_y \frac{\partial h}{\partial y} \quad (10b)$$

$$q_z = -K_z \frac{\partial h}{\partial z} \quad (10c)$$

where q_x , q_y , and q_z represent the x-, y-, and z-components of the Darcy velocity vector. Similarly, $\delta h/\delta x$, $\delta h/\delta y$, and $\delta h/\delta z$ are the partial derivatives of the total hydraulic gradient in the x-, y-, and z-directions, respectively.

Main Equations of Flow

If a small cube of the wetland were viewed, with width, length, and height of Δx , Δy , and Δz respectively, based on mass balance principles, the following flow equation can be derived (Domenico & Schwartz, 1998:60)

$$-\left(\frac{d}{dx} q_x + \frac{d}{dy} q_y + \frac{d}{dz} q_z \right) = \frac{1}{\rho_w} \cdot \frac{d}{dt} (\rho_w \cdot n) \quad (11)$$

where ρ_w is the density of water. The right-hand side of equation 11 represents the accumulation of water in our small cube of wetland over time. In this study, flow in the wetland is assumed to be steady, and therefore, we can

set the right side of equation 11 equal to zero. Applying the Darcy equation (10a - 10c), equation 11 then becomes (Domenico & Schwartz, 1998:60)

$$\frac{d}{dx} \left(K_x \frac{dh}{dx} \right) + \frac{d}{dy} \left(K_y \frac{dh}{dy} \right) + \frac{d}{dz} \left(K_z \frac{dh}{dz} \right) = 0 \quad (12)$$

Under isotropic and homogeneous conditions ($K_x = K_y = K_z$), the hydraulic conductivity can be eliminated from the equation, giving us

$$\frac{d^2}{dx^2} h + \frac{d^2}{dy^2} h + \frac{d^2}{dz^2} h = 0 \quad (13)$$

or simply

$$\nabla^2 h = 0 \quad (14)$$

Equation 14 is Laplace's equation. The solution to this equation, with appropriate boundary conditions, quantifies the value of the hydraulic head at any point in the three-dimensional flow field (Domenico & Schwartz, 1998:61).

Residence-Time Distribution Function

Probably the simplest way of characterizing the flow in a wetland is by calculating the mean residence time, or the average time that a water molecule spends in a flow domain. The mean residence time (τ) is the ratio of the

volume of water in the wetland (V) and the average flow rate (Q).

$$\tau = \frac{V}{Q} \quad (15)$$

Calculating the mean residence time in this way implicitly assumes that there are no stagnation, shortcircuiting, or dead zones in the wetland (Rash & Liehr, 1999:310).

Though the mean residence time provides a quick method of measuring the average time that water molecules spend in a wetland, it is just a single parameter and it doesn't provide much insight into actual flow behavior. Another approach is to determine the probability that a given fraction of water molecules will be in the wetland for a given time. Similar to the probability density function in statistics, the residence-time distribution function (RTDF) can be used to characterize flow through a reactor, such as the wetland (Clark, 1996:475).

The RTDF is a function of time, represented as $f(t)$. The usefulness of the RTDF is that the area under the curve can be used to predict the probability that a flowing molecule will remain in the system for a given time. Knowing the estimated residence time for molecules in a reacting system allows us to estimate the extent of reaction, so long as we are able to quantify the reaction

kinetics. Thus, in a treatment wetland, once we determine reaction kinetics the RTDF can be used to predict effluent contaminant concentration for a given influent concentration.

For a closed system, the expected RTDF may appear as shown in Figure 2-4.

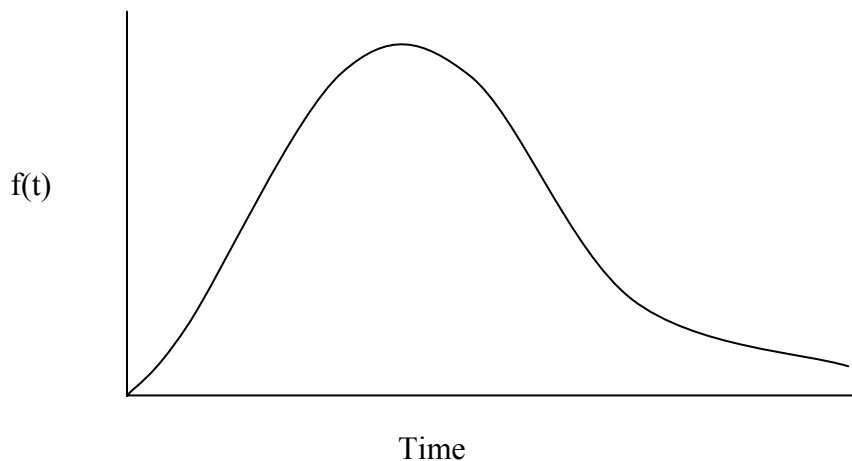


Figure 2-4 RTDF from Clark, 1996

Similar to the probability density function in statistics, the area under the curve must be 1, so equation 16 must be satisfied by the RTDF.

$$\int_0^{\infty} f(t) dt = 1 \quad (16)$$

Based on the properties of the RTDF, we find that the probability a water molecule will remain in the wetland for longer than time t_1 and less than time t_2 is:

$$\text{prob}(t_1 \leq t \leq t_2) = \int_{t_1}^{t_2} f(t) dt \quad (17)$$

An RTDF for a real system can be developed by use of a dye-tracer test. Rash and Liehr (1999) used a dye-tracer test in a study of constructed wetlands treating landfill leachate. They used Lithium as a tracer and were able to develop an RTDF to characterize the flow. Details for conducting such a test are discussed in Clark (1996:473).

When a dye-tracer test is not available, an RTDF can be developed by numerically simulating the residence times of individual molecules as they are transported through the system. To use this method, a model must be developed that reflects the flow dynamics of the wetland. The model must also have the capability to trace the paths of particles through the wetland, and provide the residence times of those particles. With this information, the residence times can be graphed to provide a cumulative RTDF. The RTDF can be derived as the derivative of the cumulative RTDF (see Figure 2-5). The more particles chosen, and the better the flow model of the system, the more accurate the RTDF will be.

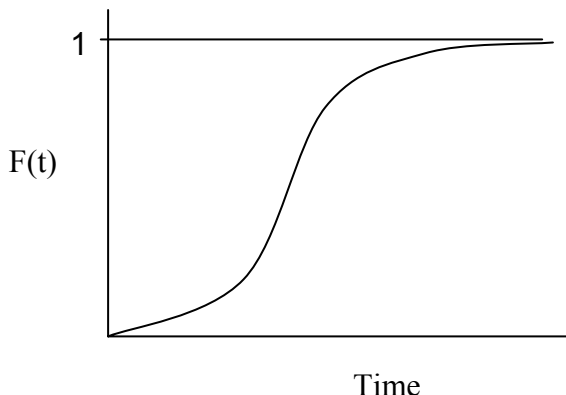


Figure 2-5 Cumulative RTDF

Mapping Groundwater Flow

By taking measurements from the piezometers installed in the wetland, the direction of flow in three-dimensions can be determined.

Flow Direction

Often, when applying Darcy's Law to determine flow, flow is assumed to be horizontal. This assumption is a simplification that is made because often the main interest in aquifer flow is how does the flow move horizontally (e.g. from a recharge or contaminant source area to a pumping well). In a wetland, however, flow may be primarily vertical. Installing piezometers at a single depth would allow us to calculate the hydraulic gradient in the x-y plane, but would not indicate whether the flow is horizontal or vertical. To overcome this, nests of piezometers can be installed. A piezometer nest consists

of multiple piezometers with nearly identical x-y coordinates, but at different depths. Using piezometer nests, we can measure hydraulic gradients in the vertical direction, which would indicate whether or not there is vertical flow.

Flow Diagram

A flow diagram is a visualization of groundwater flow using flow nets. Knowing the hydraulic head distribution in the wetland, and because water flows from high hydraulic head to low hydraulic head, flow nets can be constructed for the wetland. Flow lines are perpendicular to equipotential lines when $K_x = K_y = K_z$. Building a two dimensional flow net is as simple as connecting the points where the measured hydraulic heads are the same, then drawing lines perpendicular to indicate the direction of flow.

In some cases, the hydraulic head may be different vertically and horizontally; therefore, a three-dimensional flow net must be constructed. Building a three-dimensional flow net requires three-dimensional head data, such as can be obtained using piezometer nests, with piezometers at specific horizontal (x, y) locations installed at several depths.

Software

MODFLOW is currently the most popular software for modeling groundwater flow. Visual MODFLOW is a version of MODFLOW produced by Waterloo Hydrogeologic, Inc. that provides a three-dimensional capability. This is essential for a wetland analysis.

Required inputs for the Visual MODFLOW software are the hydraulic parameters discussed previously in this chapter. These include total porosity, effective porosity, and hydraulic conductivity. In addition, boundary conditions for head must be set. With these inputs MODFLOW solves equation 14 for the hydraulic head at various points in the wetland, and as discussed in the previous section, applies Darcy's Law to calculate groundwater velocity throughout the wetland.

$$\nabla^2 h = 0 \quad (14)$$

III. Methodology

Overview

To gather data for analysis in the wetland cell, a grid of equally spaced piezometers was installed. To construct a three-dimensional picture of the flow, the piezometers were driven into each of the three layers of the wetland at each grid point. Measurements of the water height in the piezometers were used later for comparison with the heads simulated by a numerical model of the wetlands system.

Conducting slug tests with monitoring wells provided a means for estimating the hydraulic conductivity. Soil samples were taken and analyzed for estimating porosity and effective porosity. These parameters were then applied to a computer model to simulate the groundwater flow and to build a Residence Time Distribution Function (RTDF).

Sampling Grid

Sixty-six nests of Model 615 Solinst Drive-Point piezometers with shields were installed equally spaced throughout the wetland in the summer of 2002 (see Figure 3-1). Along the length of the wetland are 6 rows and 11

Wetland Cell #2

A: Top Layer
B: Middle Layer
C: Bottom Layer

(A) (C)
 (B)

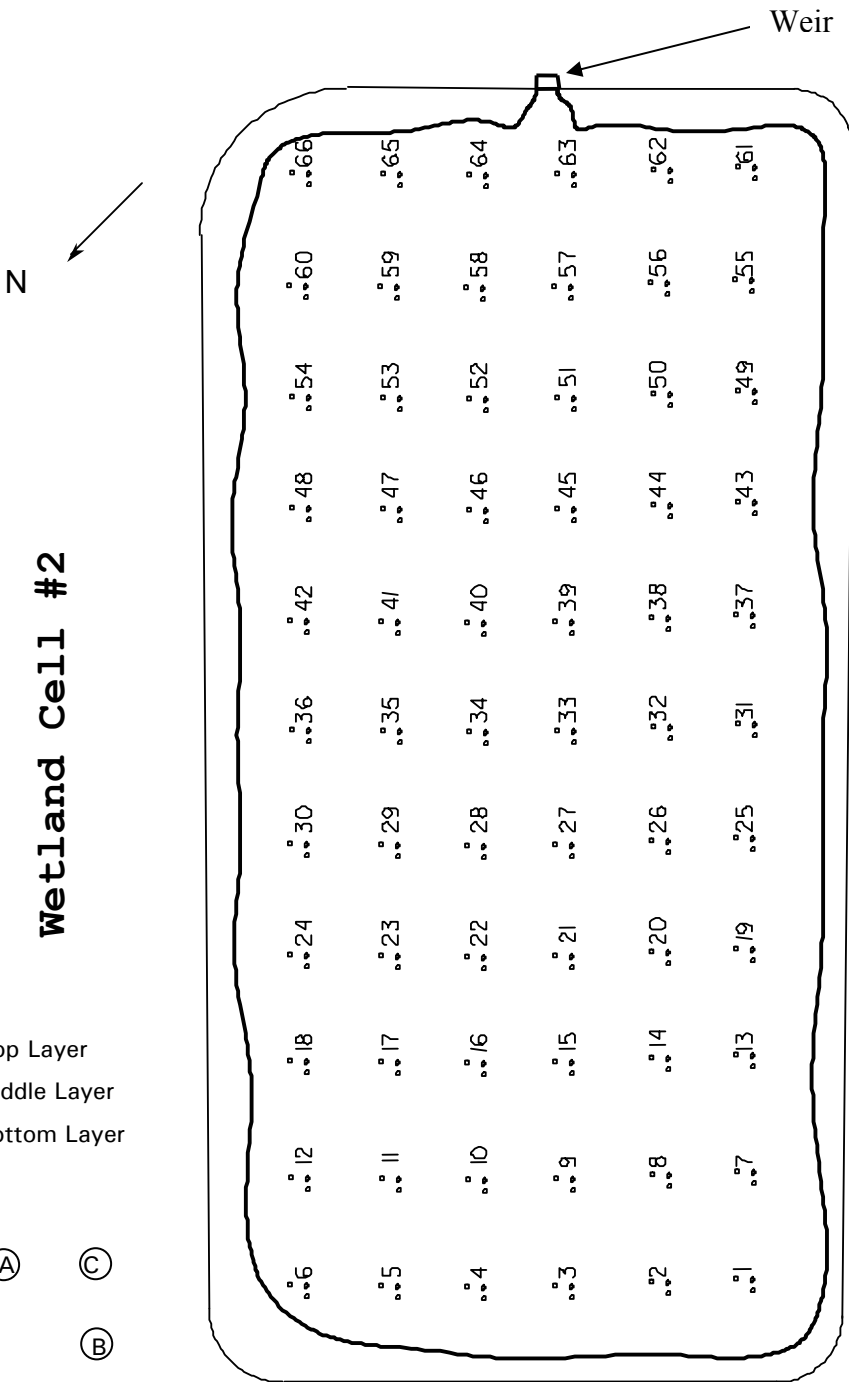


Figure 3-1 Piezometer Placements

columns. Each nest consists of three piezometers, for a total of 198 piezometers. The piezometers inside the nest are all one foot apart. Nests of three piezometers were

installed to better understand the flow through each of the three layers in the wetland.

Piezometer Installation

The installation of the piezometer involved three main steps: inserting, sealing, and development.

Insertion

Before installing the piezometers, surveyed stakes were put in place to build a grid with strings that has intersections equally spaced apart. The intersections of string within the grid provided guidance for placement of the piezometers. Once the grid was in place, the piezometers were assembled. Each piezometer consisted of a shield, a screen, $\frac{3}{4}$ inch stainless steel pipe, $\frac{3}{4}$ inch galvanized steel riser, and a $\frac{1}{2}$ inch Teflon-lined tube.

Stainless steel pipes were used in order to prevent corrosion of the pipe inside the wetland. The galvanized steel risers were used instead of stainless steel to save on cost since corrosion does not matter above the ground. Each piezometer was driven down to one of the three layers, and then pulled back out 6 inches to allow the screen to separate from the shield. The method of driving the piezometers was by first attaching a steel pipe with a flat top to the piezometer. A hand-held slide hammer was then

placed over the steel pipe and used to drive the piezometers into the ground. Figure 3-2 is a picture of a piezometer being driven into the ground by this method.



Figure 3-2 Driving Piezometers with a Slide Hammer

Before driving the piezometers, tape was used to mark the proper distance to drive the piezometer down for the screen to be in the center of the desired layer once retracted and in place. Figure 3-3 shows a profile view of the placement of the piezometers, along with a label for each of the components.

Water Seal

Driving a piezometer down to the various layers provides a pathway for the water that is under pressure to travel to the surface via the sides of the piezometer. To keep water from "leaking" out, each of the piezometers must be sealed. The method for sealing the piezometers is by packing bentonite around where the piezometers come out

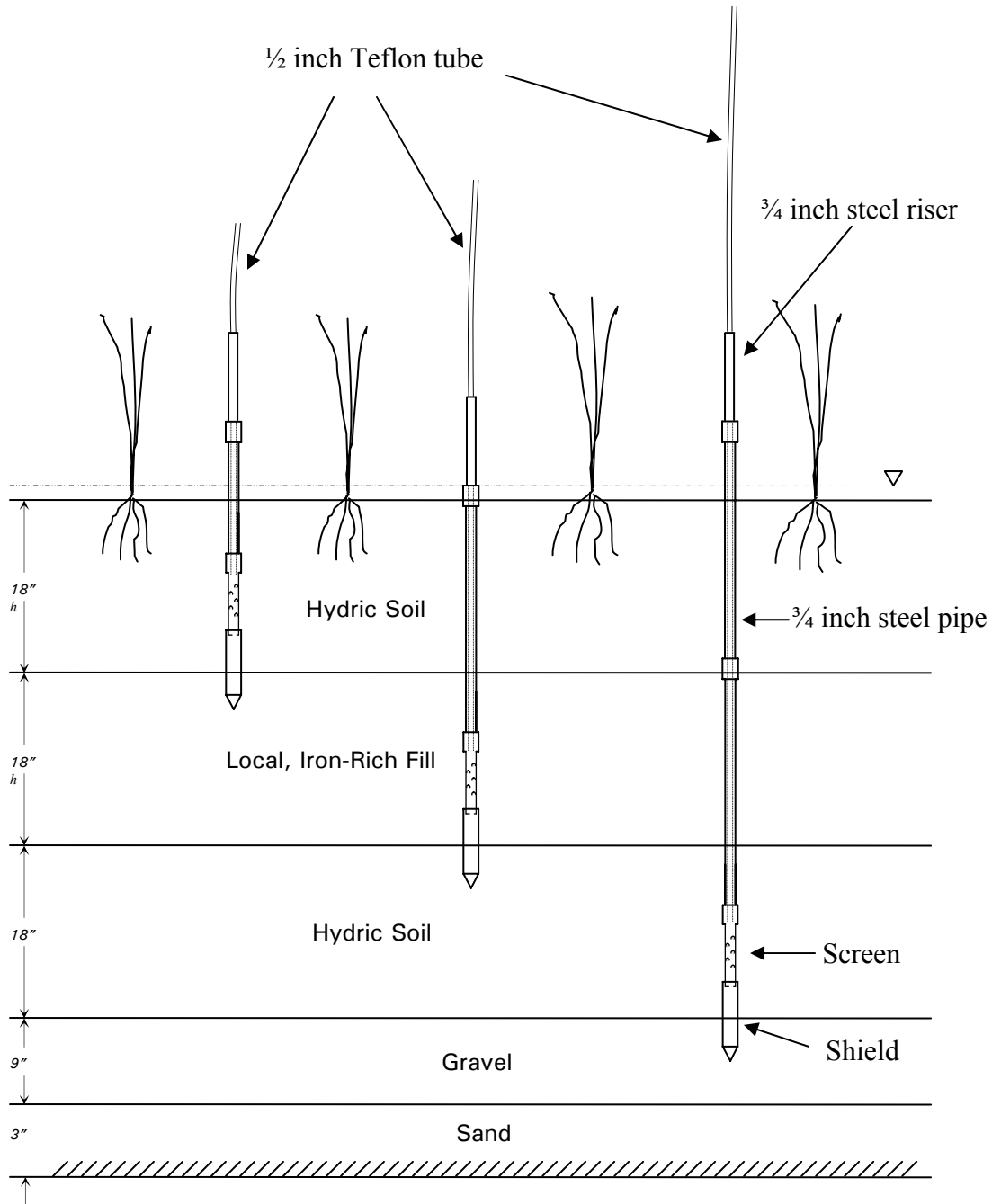


Figure 3-3 Piezometer Placement Cross-section

of the ground. To accomplish this, dirt was removed from the surface of the wetland around each of the piezometers to about 4 inches deep, clearing a space around the piezometer about 1 inch thick. This space was then filled

with bentonite, which expanded on contact with water. The expansion provided the necessary seal so that water could not bypass the wetland along the piezometers. Figure 3-4 provides a visual representation of the bentonite in place.

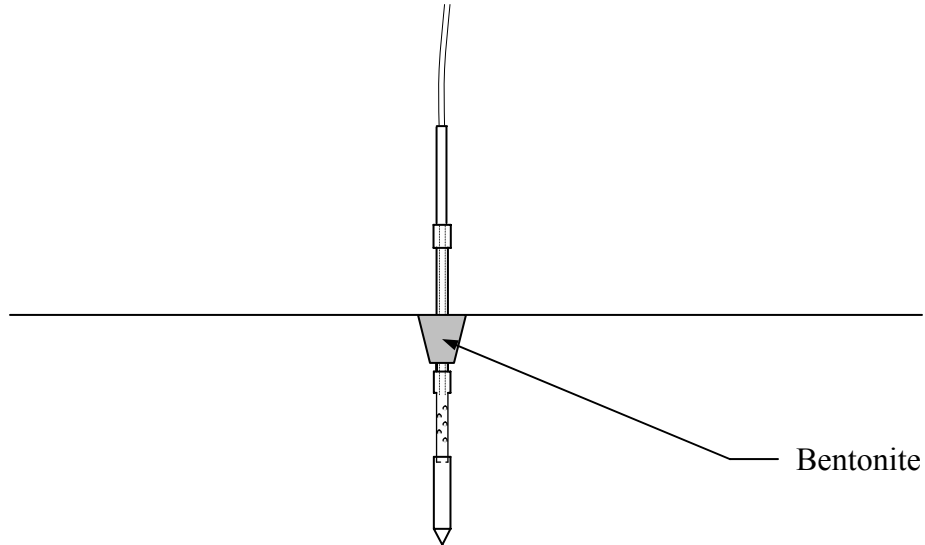


Figure 3-4 Bentonite Placement Diagram

Development

Once the piezometers are driven and sealed, there still may not be water rising up the pipe. This can be because either the screen is clogged with sediment or there is a pocket of air at the bottom of the piezometer. To fix this problem, each piezometer must be developed.

The method of development is using a Solinst Model 410 Peristaltic Pump to pump water into the piezometer, and then back out again repeatedly. Pumping water in and out of the piezometer clears the screen of any clogging by sediments, as well as removes air that may be trapped

within the soil layer. This method creates the ability to obtain an accurate potentiometric head measurement, as discussed next.

Piezometer Measurements

Water level measurements were taken in the $\frac{1}{2}$ " Teflon tubes in each of the piezometers. A ruler was used for measurement of the water level above the top couplings within $1/16^{\text{th}}$ of an inch. The head is then calculated by adding the height of the water level measured by the ruler to the elevation of the coupling. The majority of the piezometers in the bottom layer had a water level below the ground surface; therefore, the water level was measured using a Solinst Model 101M Water Level Meter for the bottom layer piezometers, as well as others that were below the surface. The Solinst Meter is a device that beeps when the measuring tape encounters water when placed down the Teflon tube. This gives a measurement of the distance that the water level is from the top of the Teflon tube. The head is then calculated by subtracting the difference between the water level and top of the Teflon tube from the elevation of the top of the Teflon tube.

Once each of the measurements was taken, they were adjusted to a common datum. The datum chosen was the rough

estimate of the location of the bottom liner. Survey data of the three-dimensional coordinates of each piezometer coupling was gathered from the Civil Engineer personnel of the 88th Air Base Wing, Wright-Patterson Air Force Base, by use of Global Positioning System (GPS) equipment. The global coordinates were given to the nearest 1000th of a foot. Since the wetland is about 5 feet, 9 inches deep, the liner was estimated to be 6 feet under the elevation of the piezometer coupling 1C. The extra three inches of depth takes into account the height of that piezometer coupling above the ground level. Once the elevation of each of the piezometer couplings was determined, the water level measurement was added to the coupling elevation to determine the total head.

Water level measurements were taken on three separate occasions throughout November 2002, using the same flow rate in order to find an average of the measurements. An average of three measurements helps to decrease error since the measurements differ up to one inch from day-to-day depending on the barometric pressure.

Groundwater and Soil Parameters

Before a model can be built, additional parameters must be obtained. The primary parameters that must be determined are the porosity, effective porosity, and the hydraulic conductivity.

Porosity/Specific Yield

To measure the porosity, a sample core was removed from the wetland for analysis. To remove a core sample, a 2-inch diameter aluminum irrigation pipe was first driven into the ground with a sledgehammer. The pipe was then withdrawn by a pulley system with a hand crank on a tripod placed above the pipe. To prevent losing the sample, a vacuum was created with a plunger inside the pipe that moves up the pipe with the soil as the pipe is driven into the ground. The entire depth of the wetland cannot be removed in one core sample because there is too much resistance after about 20 inches of depth. Once a depth of 20 inches is reached, the top of the pipe begins to collapse from the sledgehammer. Therefore, only about 16-24-inch cores were taken at a time until the depth of the wetland was removed. Once the pipe is extracted, aluminum foil is placed over the end to hold the sample in place and to keep from losing water due to evaporation. The core sample was then transferred to the laboratory for analysis.

To remove the core, the pipe was sawn length-wise with a skill saw, and then peeled apart.

Once the core sample was removed from the pipe, a measured volume of soil (roughly 1 Cubic Inch) was taken from sections of the core every 10 centimeters. The volume of soil was sliced out of the 10-centimeter section using a serrated knife to avoid compressing the sample. The sample cut from the core was then transferred by hand and weighed on a Mettler TL 1200 scale to the nearest 100th gram. The soil weighed was assumed be completely saturated, with the loss of water due to evaporation or other means being minimal. The weight of the volume of the saturated soil is the "wet weight."

To calculate the porosity, the wet and dry weights are needed. However, before the dry weight is obtained, the soil is drained in order to calculate the specific yield and to ultimately estimate the effective porosity. The specific yield is the amount of water that can be removed from a sample due to draining by gravity. After the initial weight of the soil was acquired, it was set-aside on a screen, fully enclosed for 72 hours. The screen allows the soil to drain, while the enclosure prevents loss of water due to evaporation.

After draining for 72 hours, the samples were weighed once more for the "drained weight." Using the initial wet weight and the drained weight, the specific yield of the soil can be calculated as follows:

$$S_y = \frac{(W_{sample} - W_{gravity\ drained})/\rho_{water}}{V_{sample}} \quad (18)$$

The effective porosity is defined as the percentage of interconnected pore space (Domenico & Schwartz, 1998:14). The value for effective porosity can be very similar to the specific yield, but is always higher due to the capillary forces that keep some water from draining out of a sample. As noted in Chapter 2, effective porosity is a function of the hydraulic gradient, and the higher the gradient, the closer the values of effective porosity and total porosity. For fine-grained sediments (such as found in the wetland) the effective porosity is much closer to the specific yield than the total porosity. Therefore, the specific yield is used to approximate the effective porosity.

Knowing the weight of the drained sample, it is now necessary to measure the sample dry weight for use in determining total porosity. The dry weight results from taking the sample and placing it into an oven at 105 °F until a constant weight is obtained. The constant weight is considered the dry weight of the sample. The total

porosity is given in equation 8 as the ratio of the volume of the voids to the total volume of a sample. The total volume of the sample has already been measured. To find the volume of the voids, the following equation can be used:

$$V_{\text{voids}} = \frac{W_{\text{wet}} - W_{\text{dry}}}{\rho_{\text{water}}} \quad (19)$$

where ρ_{water} is the density of water, or 1 g/cm³.

Hydraulic Conductivity

The method chosen for measuring the horizontal hydraulic conductivity of the three layers was the Hvorslev method (Domenico & Schwartz, 1998:116). The Hvorslev method is widely used in field practice to interpret slug injection tests. Slug injection tests involve inserting a slug of known volume into a well and measuring the drop in head over time.

In the fall of 2002, 6 nests of wells were placed in each wetland. These nests were similar to the piezometer nests in that each had three wells, one well for each layer. The 2-inch diameter wells were made from PVC and have 5-inch screens. The locations of the nests can be seen in Figure 3-5.

Wetland Cell #2

- A: Top Layer
- B: Middle Layer
- C: Bottom Layer

(A) (C)
 (B)

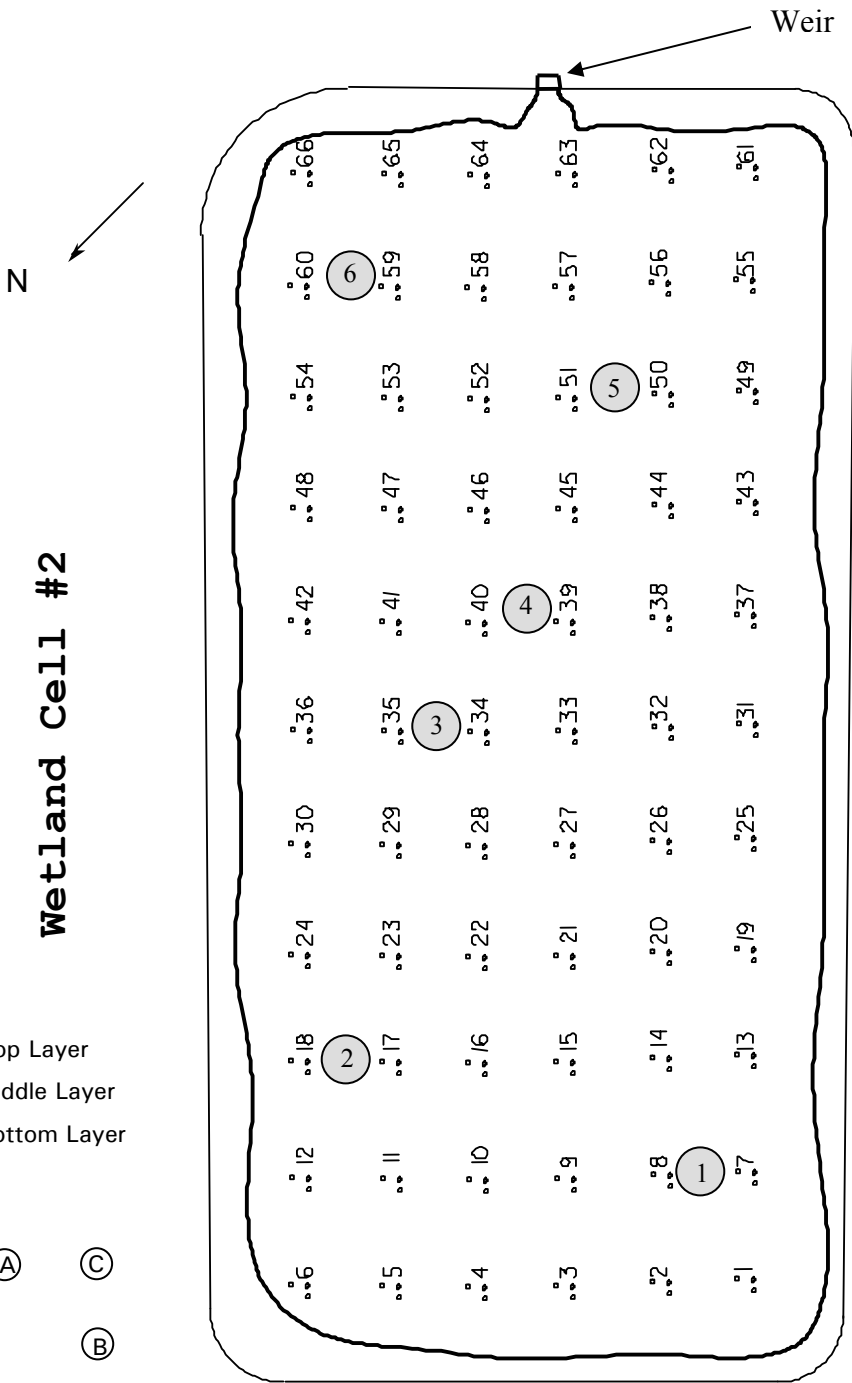


Figure 3-5 Locations of Well Nests

To apply the Hvorslev method to the wetland, the 6 nests of wells were used for slug injection tests. The

size of the slug chosen depended on how much water the well could hold. The wells in the upper layer tended to be the shortest, therefore only a $\frac{1}{2}$ -Liter slug of water was used. The middle layer well could hold about 1 Liter and the bottom layer about 2 liters. Before pouring slugs into wells, the distance from the top of the well to the water surface must be measured. This measurement is the pre-slug depth and is used later for calculations of hydraulic conductivity. Once a slug was poured into the well, the distance was immediately measured with the Solinst Model 101M Water Level Meter from the top of the well to the water surface and recorded as the first measurement at a time of 0 seconds. As the water receded back into the ground, measurements were taken and recorded along with their respective time from the first measurement.

Once the data were collected from slug tests at all 18 wells, the Hvorslev equations were applied. Hydraulic conductivity can be determined using the Hvorslev equation as follows (Domenico & Schwartz, 1998:116):

$$K = \frac{A}{F \cdot (t_1 - t_2)} \cdot \ln\left(\frac{h_1}{h_2}\right) \quad (20)$$

where A is the area of the monitoring well and F is a shape factor that depends on the screen size. h_1 and h_2 are the depths of the water in the well measured upwards from the

pre-slug depth at their respective times, t_1 and t_2 . The shape factor can be derived from the equation,

$$F = \frac{2\pi L}{\ln\left(\frac{L}{r}\right)} \quad (21)$$

where L is the length of the screen and r is the radius of the well. This shape factor applies for $L/r > 8$. With the 5-inch screen and the 1-inch radius, the L/r in this case is 5. The shape factor in equation 22 will still be used, however, since we only hope to obtain an approximation of hydraulic conductivity and using this method provides a very convenient method of approximation.

The above equations were used to interpret those pump tests where the rate of receding water was so quick so as to allow gathering only a few head measurements, amounting to about half of all the pump tests. When possible, to get a more accurate approximation of hydraulic conductivity, it is best to take multiple measurements between the initial time of injecting the slug and the final time at which the water returns to the pre-slug depth. With many measurements of head, it is possible to rearrange the equations to find the hydraulic conductivity by the trend of the data.

For a borehole area of πr^2 , equations 20 and 21 can combine to form

$$K = \frac{r^2 \cdot \ln\left(\frac{L}{r}\right)}{2 \cdot L} \cdot \frac{\ln\left(\frac{h_1}{h_2}\right)}{(t_1 - t_2)} \quad (22)$$

To simplify further, take $h_1 = h_0$, at $t = 0$ and $h_2 = 0.37h_0$ so that

$$\ln\left(\frac{h_1}{h_2}\right) = \ln\left(\frac{h_0}{0.37h_0}\right) = \ln(2.7) = 1.0 \quad (23)$$

Equation 23 then becomes

$$K = \frac{r^2 \ln\left(\frac{L}{r}\right)}{2 \cdot L \cdot T_0} \quad (24)$$

where T_0 is the time intercept on the pump test head versus time field curve where the ratio $h/h_0 = 0.37$. To find T_0 , the logarithm of h/h_0 is plotted versus time, and a best straight-line fit to the data. An example of this graph is in Figure 3-6. In this example, T_0 is roughly 100 seconds at $h/h_0 = 0.37$. The hydraulic conductivity would then be

$$K = \frac{1^2 \cdot \ln\left(\frac{5}{1}\right)}{2 \cdot 5 \cdot 100} = 1.61 \cdot 10^{-3} \text{ Inches/Second} \quad (25)$$

with a well radius of 1 inch and screen length of 5 inches.

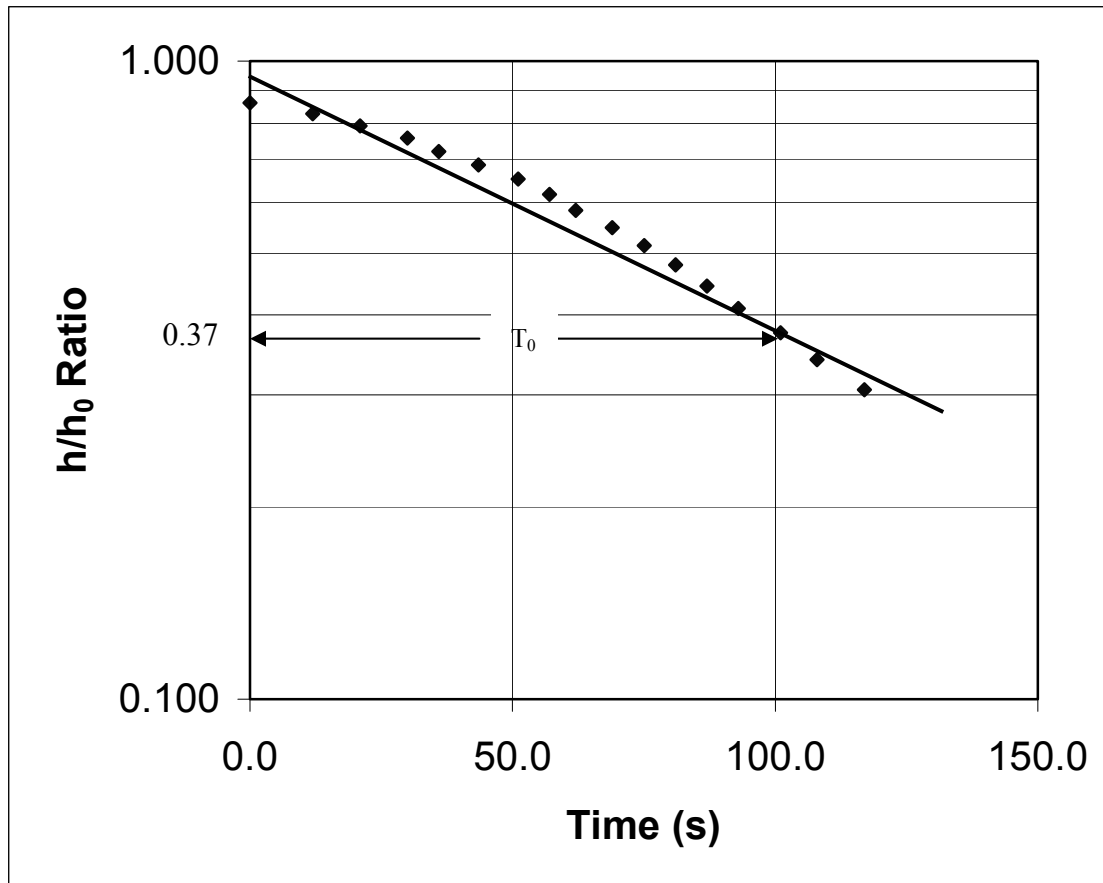


Figure 3-6 Field Response of a Slug Test

Numerical Model

The three-dimensional numerical model was developed using Visual MODFLOW® by Waterloo Hydrogeologic, Inc. To mimic the wetland, the model was set up using the layers of soil as seen in Figure 3-3. Each layer of the model was broken into 1.5 ft x 1.5 ft cells in order to provide for an accurate representation of the shape of the wetland and a better distribution of the hydraulic conductivity, which

is assumed different both horizontally and vertically throughout the wetland.

The piezometers were input into the model as observation wells and were placed according to their location from the survey. The data from the survey were given in global coordinates from a GPS system. The coordinates were then transferred to a local coordinate system with the x-axis paralleling the long side of the wetland. The first piezometer, 1B, was assigned the x and y-coordinates in feet of (10.0, 15.0). All other piezometer locations were based on the x- and y-coordinates of this first piezometer. The x-axis was drawn along a straight line between piezometer 1B and 60B.

The elevation of each of the piezometers was also initially given in global coordinates. To transfer these elevations to local coordinates, the liner was chosen as a baseline for the zero elevation. The coupling on the first bottom-layer piezometer, 1C, was assigned an elevation based on its vertical distance above the liner. All other elevations of piezometer couplings were then calibrated to that first coupling's vertical coordinate. The elevation of the screen at the bottom of each of the piezometers was calculated by subtracting the length of each piezometer from the elevation of the coupling.

Parameter Input

Once the piezometers were in place in the model, soil parameters were assigned to each layer. The total and effective porosity used in the model were determined from the core sample for each layer. It was assumed that total and effective porosity was the same throughout each layer, while the horizontal conductivity varied throughout the layer, as discussed next.

Six horizontal hydraulic conductivities were assigned for each of the three layers. In order to input the hydraulic conductivities into the model, the six values were interpolated by kriging. The conductivities, along with their coordinates, were interpolated with a FORTRAN code written by Huang (2002), using Compaq Visual Fortran software. The output to this code produced 18 values of conductivity for each layer, evenly distributed. Having 18 values of conductivity is a better distribution for the model than six. The 18 sections of each layer were assumed isotropic and homogeneous within the bounds of the section. Therefore, the vertical and horizontal conductivities were input the same for each section.

The input of flow of the water into the model wetland was represented by a total of 120 injection wells with flow rates that all add to 15 GPM. To mimic the three

perforated pipes, 40 injection wells were placed in a straight line along the estimated location of each of the 3 inlet pipes. Figure 3-7 provides a representation of the model input showing the injection wells.

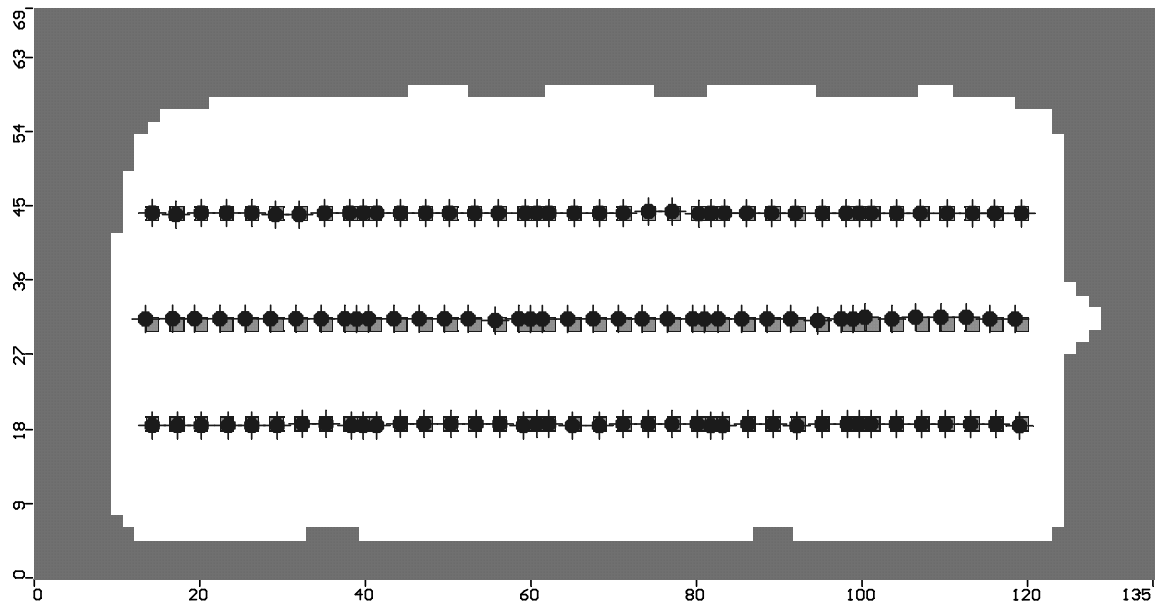


Figure 3-7 Injection Wells—Top View

For the outlet of the flow, a "dummy" layer was placed above the top layer of soil to represent the water. The hydraulic conductivity of this layer was assigned the value of 1 ft/s so that there would be very little resistance to the inflow of water into the layer. To mimic the water that is on top of the soil, a constant head boundary was specified at the weir location allowing water to flow out of the model at that height.

Running the Model

The MODFLOW software gives a choice of 4 solvers to solve the flow equation discussed in the previous chapter. The one chosen for this model is the Preconditioned Conjugate-Gradient Package (PCG2). The PCG2 solver can simulate linear and non-linear flow conditions and its convergence is dependent on the head change and residual criteria (USGS, 1990). Using 100 outer iterations and 40 inner iterations was sufficient for convergence to a solution.

For the purpose of the model, the first layer (the layer representing water at the wetland surface) was modeled as unconfined, with variable transmissivity. Transmissivity is defined as the product of the hydraulic conductivity and the saturated thickness. Allowing the transmissivity to vary allows for the water level of the top layer to vary. This reflects the real wetland, where the water on top of the wetland varies from 0 to about 8 inches deep. The remaining soil layers were modeled as confined.

Once these parameters were set, the model was run for MODFLOW and MODPATH. The MODPATH option allows preset particles to be transported through the wetland for use in determining residence times and path direction.

Model Output

MODFLOW outputs contour plots of head equipotentials, velocity and flow direction vectors, and path lines. MODFLOW also will compare modeled versus observed heads (piezometer measurements). Input parameters (conductivity, constant head boundary condition values, etc.) can be adjusted until calculated heads approximate the observed heads. The hydraulic parameters will not be used as fitting parameters in this study since the conductivity, specific yield, and total porosity values have all been independently measured, as described previously. The constant head boundary condition assigned at the weir, however, can be used as a fitting parameter to fit the modeled heads to the heads measured by the piezometers.

Residence Time Distribution Function (RTDF)

To build an RTDF as discussed in Chapter 2, the first step is to collect residence times of individual water molecules in the wetland. For water molecule residence times, the water molecules have to be tracked from the point of injection into the wetland. The tracking of molecules can be achieved through MODPATH by placing a molecule at a given point in the wetland. To imitate the initial location of water molecules entering the wetland,

180 water molecules were placed inside the injection wells discussed previously. The path chosen by molecules is very location-specific. Therefore, three molecules were placed in alternating injection well cells in a layer that is in the vertical center of the injection wells (see Figure 3-8). With all of the water molecules in place, MODPATH was run to provide path lines of the molecules.

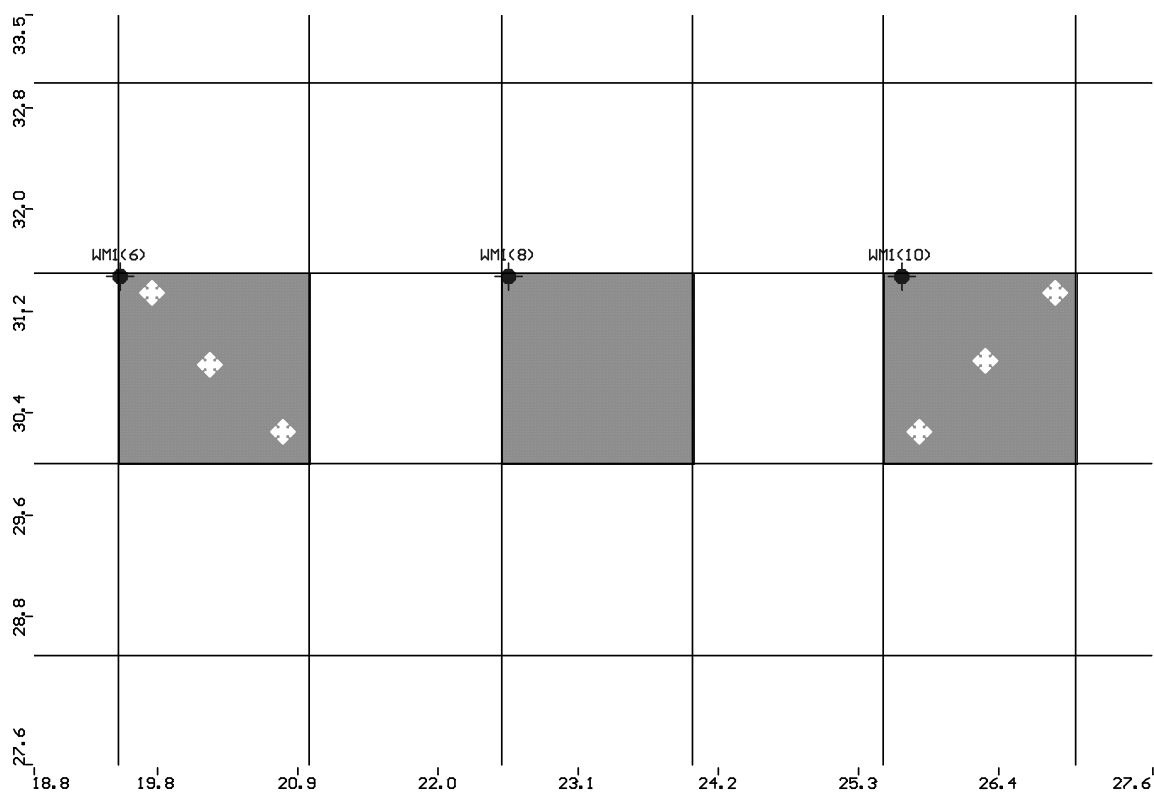


Figure 3-8 Particle Locations in Three Adjacent Injection Cells

To determine the RTDF, the number of molecules exiting the wetland in a given time increment must be known. In the MODFLOW output, the model running time can be set and adjusted. To find the number of molecules leaving the

wetland in specific time increments, the running time of the model had to be gradually increased by the time increment chosen, while simultaneously counting molecules leaving the wetland between time steps. The data collected through this process can be used to build the cumulative RTDF.

The cumulative RTDF can be approximated as a graph of the cumulative number of molecules leaving the wetland versus time. This function, $F(t)$, is normalized by dividing the number of molecules exiting the wetland by the total number of molecules being observed, so as time gets large, the value of $F(t)$ approaches 1.

Once graphed, the cumulative RTDF can be used to find the RTDF, $f(t)$, by taking its derivative. To find the derivative of $F(t)$, we can use Excel to fit the $F(t)$ points with a polynomial, and then take the derivative of the polynomial.

Knowing the RTDF, the mean residence time, τ , can be calculated as

$$\tau = \int_0^{\infty} f(t) \cdot t \, dt \quad (26)$$

The mean residence time calculated using equation 26 (and which is based on the flow model of the wetlands) could be

compared to the Theoretical Mean Residence Time calculated using the equation

$$\tau = \frac{V}{Q} \quad (15)$$

which is based on the actual volume of water in the wetland and flow through the system.

IV. Results

Piezometer Installation

All 198 piezometers were installed successfully between July and August 2002. Each was driven 6 inches beyond the desired depth, and then extracted 6 inches to separate the shield from the screen. Once in place, bentonite was emplaced at the surface around the piezometer pipes to provide a seal. During initial installation of some of the piezometers, it was observed that the water pressure below the bentonite seal was too great, and the seal was broken. The problem was due to using fine-grained bentonite, which resulted in a very soft seal. To solve the problem, the fine-grained bentonite was replaced with a gravel bentonite on all of the piezometers. Few leaks were found after this solution was implemented. The leaks that were observed were dealt with individually.

Once the piezometers were sealed and developed, all except three of them had hydraulic head readings. Most of the top and middle layer piezometers indicated a head that was above the ground surface. The bottom-layer piezometers seemed to have a low hydraulic head reading, below the ground surface, indicating that water would be flowing down toward the bottom layer, rather than up as expected. The

first attempt to fix this problem was for all of the bottom-layer piezometers to be developed. Development of those piezometers still did not result in the expected hydraulic head measurements. Most of the hydraulic head readings in the bottom layer piezometers were just below the ground surface, while the top and middle-layer piezometers were above the ground. For lack of another solution, the bottom-layer piezometers were left alone until data could be gathered and analyzed in hopes of developing inferences about the reason for the low hydraulic head. Some middle and top-layer piezometers were developed, mostly on an individual basis. To check if a screen was plugged, water could be sucked up the tube, and then released to settle back to its original position. If the water returned to its original position relatively quickly, then the screen was assumed to be clear.

Piezometer Measurements

All but three piezometers had sufficient water in them to measure the hydraulic head. The three piezometers without water were all in the bottom layer. All head measurements are annotated in Appendix A.

The average head measurement, using the liner as a baseline, was 4.7 feet in the top layer and 5.1 feet in the

middle layer, indicating upward flow from the middle to the top layer. The bottom layer, on the other hand, had an average head measurement of 4.0 feet, which would indicate downward flow from the middle layer to the bottom layer. Downward flow was not expected and is discussed further in the next section.

Explanation for Unexpected Piezometer Head Measurements

One possibility for the lower-than-expected head readings in the bottom layer is that there were leaks in the bentonite seals around the piezometers screens. Much time was spent adding bentonite and trying to find any other possible leaks in the wetland, but no additional leaks were found.

Once all of the hydraulic head measurements were taken, the next step was to take a core sample in order to determine porosity. After reaching a depth of 48 inches with the 2-inch pipe, the core was removed. At the bottom of the core sample, a piece of liner was found. This indicated that the liner was not 66 inches down from the surface as originally planned, but at 48 inches instead. After analyzing the core sample, each of the three layers of soil were found to be 12 inches thick instead of 18 inches, accounting for the 18 inch difference between the

design depth of the liner and the apparent actual depth (66 minus 48).

There are many implications to this discovery. All of the bottom-layer piezometers were driven to 54 inches in order to have the screen centered at 45 inches once extracted 6 inches. This means that all 66 bottom-layer piezometers have breached the liner and now sit just 3 inches above the liner, most likely in gravel. With 66 holes in the liner, the apparent downward flow is explained by water leaking out under the wetland at a rate consistent with the water head established upon wetland saturation. Not all flow is downward, however, or there would be no flow of water out the weir. In about 8 nests of piezometers, the head reading in the bottom layer was greater than that of the middle layer. In Figure 4-1, the white areas indicate areas of upward flow, which are inferred from the head readings on the piezometers.

The rate of leakage can be found by subtracting the flow coming out of the weir from the inflow rate. The inflow rate was set at 15 gallons per minute for taking the hydraulic head readings. By using a bucket and a stopwatch, the flow of water coming out of the weir was measured at about 5 gallons per minute. This indicates

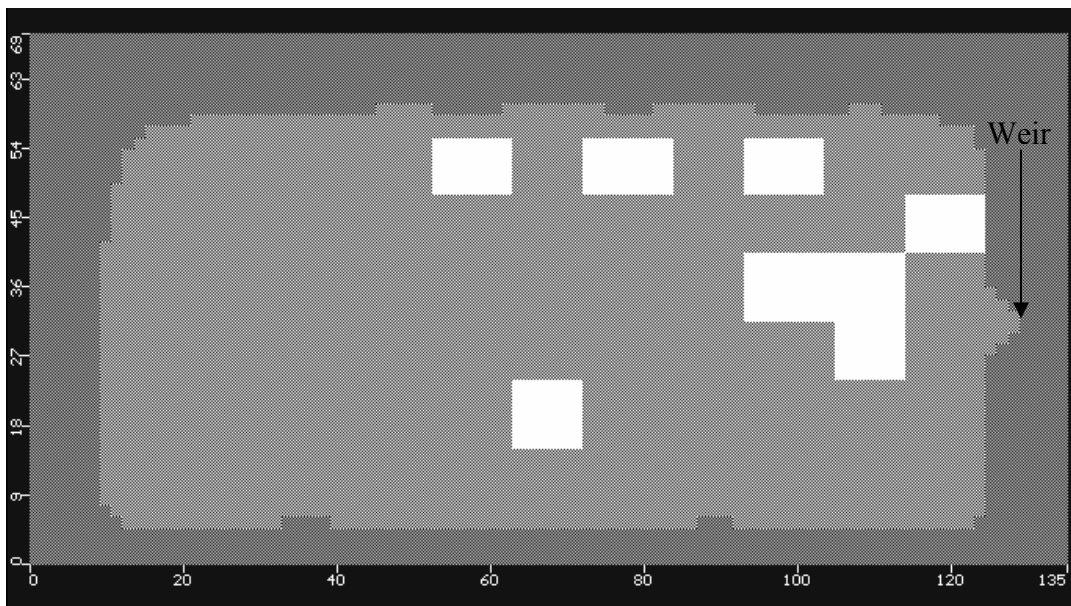


Figure 4-1 Areas of White Showing Upward Flow

that about 2/3 of the flow entering the wetland is either leaking out the bottom or lost to the atmosphere. Water lost to the atmosphere can occur from the water and soil (evaporation) and from the emergent portions of the plants (transpiration). The combination of the two processes is evapotranspiration (Kadlec & Knight, 1996:182-3). The evapotranspiration rate is minimal, attributing to removing around 1% of the inflow, and will therefore be ignored in this study.

With only 12-inch layers, the locations of the piezometers are not actually in the presumed layers. Instead, the middle-layer piezometers are in the third layer of soil, while the bottom-layer piezometers are in the gravel/sand layer as seen in Figure 4-2.

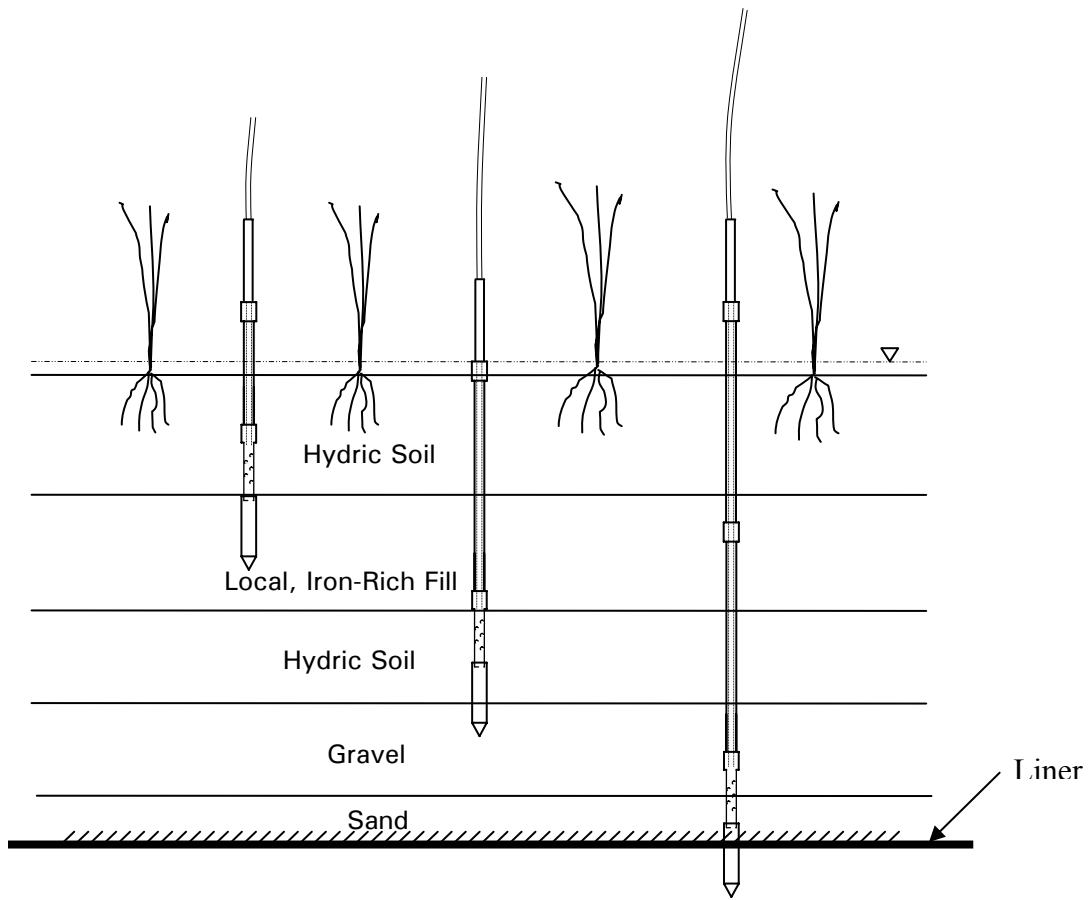


Figure 4-2 Actual Piezometer Placement Cross-section

The water leaking out of the bottom of the wetland is technically in violation of the Permit-to-Install (PTI) issued by Ohio EPA. In essence, contaminated water is being pumped from the groundwater source into the wetland and then released back into the ground (recharging the same groundwater upstream of the extraction well) without a permit to do so. Therefore the wetland cell was shut down as of 12 December 2002. Even though the wetland was shut down, enough data were collected beforehand in order to

continue with the analysis of the cell, with the assumption that all piezometers in the bottom layer are above the liner.

Parameter Estimation

The soil parameters needed for building a numerical model are porosity, specific yield, and hydraulic conductivities.

Porosity and Specific Yield/Storage

The porosity and specific yield measurements were computed from the core sample taken in December 2002 between piezometer nests 46 and 52. The results are in Table 4-1, with additional details found in Appendix B.

Table 4-1 Porosity and Specific Yield Data

Layer	Specific Yield	Porosity
Top	0.060	0.274
Middle	0.113	0.230
Bottom	0.132	0.250
Gravel	0.250	0.300

Hydraulic Conductivity

The hydraulic conductivities throughout the wetland were found by conducting slug tests, as described in Chapter 3, using 2-inch diameter monitoring wells. The data collected for the slug tests, along with the graphs for each well, are in Appendix C. Table 4-2 shows the

results of the hydraulic conductivity calculations in feet per second at the six locations shown in Figure 3-4.

Table 4-2 Hydraulic Conductivities (ft/s)

	1	2	3	4	5	6
Top Layer	0.002002	0.002682	0.000117	0.000131	0.000192	0.002482
Bottom Layer	0.001739	0.009539	0.022747	No Data	0.001127	0.001341
Gravel Layer	0.000671	0.000279	0.000447	0.002682	0.000081	0.000984

The hydraulic conductivity could not be calculated for the middle layer because of the misplacement of the 2-inch monitoring wells due to the mistaken assumption that layers were 18 inches thick, rather than 12 inches. Without an accurate way to measure the middle-layer conductivity, it could be used as a fitting parameter for calibration of the numerical model (discussed later). The gravel layer measured conductivities seem to be lower than expected. One possibility is that the screens on the six monitoring wells used for the slug test in the bottom layer could have been partially under the wetland liner in soil that has a low conductivity.

Numerical Model

When the hydraulic conductivities were applied to the FORTRAN code as described in the previous chapter, the 18 new conductivities were provided and are seen in Table 4-3.

Table 4-3 Model Hydraulic Conductivities

	Top Layer (ft/s)	Bottom Layer (ft/s)	Gravel Layer (ft/s)
1	0.001233	0.008788	0.001020
2	0.001027	0.007292	0.000832
3	0.001267	0.007299	0.000857
4	0.001267	0.007299	0.000857
5	0.000730	0.007299	0.001049
6	0.000730	0.007299	0.001049
7	0.001233	0.007299	0.001020
8	0.001024	0.007299	0.000832
9	0.001267	0.007299	0.000857
10	0.000855	0.007299	0.001310
11	0.001121	0.007299	0.000895
12	0.000730	0.008688	0.001049
13	0.001233	0.007299	0.001020
14	0.001033	0.007305	0.000832
15	0.001267	0.007299	0.000857
16	0.001267	0.007299	0.000857
17	0.001121	0.007299	0.000895
18	0.000730	0.008688	0.001049

The conductivities were applied to the model as seen in Figure 4-3. Each block represents one of the 18 measurements in the top layer from Table 4-3.

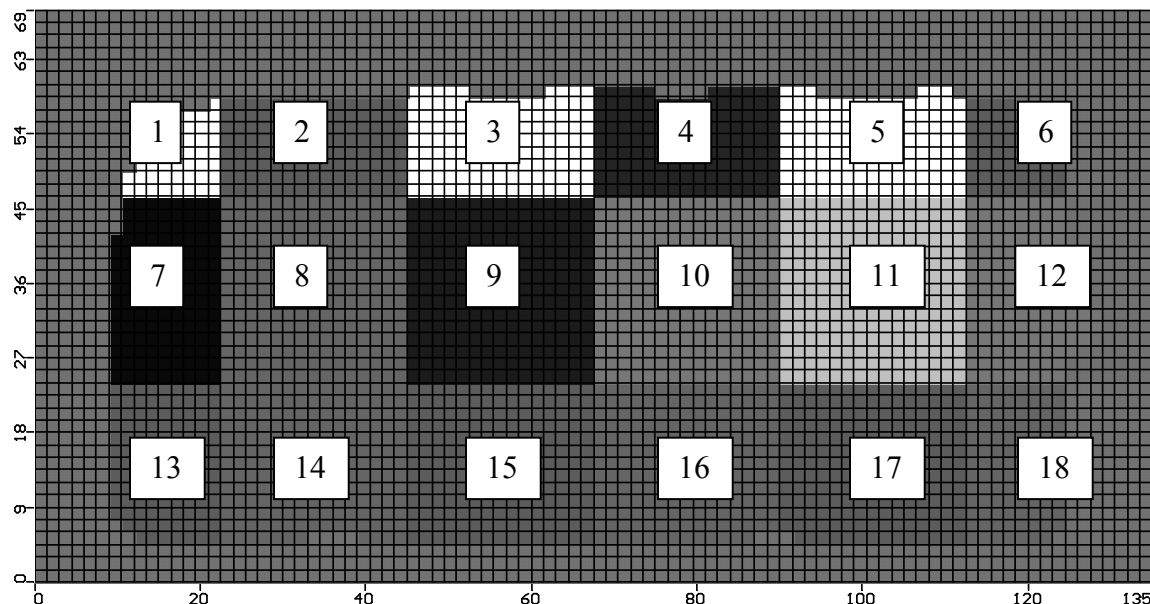


Figure 4-3 Hydraulic Conductivity Example

The other hydraulic parameters were input into the model as required. The effective porosity was estimated as the specific yield.

In building the model, the leaks in the liner had to be taken into account. Since 2/3 of the flow was leaking out the bottom of the wetland, the model had to reflect water exiting the bottom at 10 GPM. To build this into the model, a model layer was constructed to represent the leaking liner. This "liner" layer is 0.1 feet thick, with large values of horizontal hydraulic conductivity and a very small value of vertical conductivity. The hydraulic conductivity values provide a good representation of a liner by allowing water to flow within the layer, but not into the layer from the rest of the wetland. 66 extraction wells were inserted into this liner layer, each at the location of one of the 66 bottom-layer piezometers. See Figure 4-4 for the location of the extraction wells. The total flow out of the liner layer extraction wells was set at 10 gallons per minute (GPM), each with a pumping rate of -0.15 GPM, or 10/66.

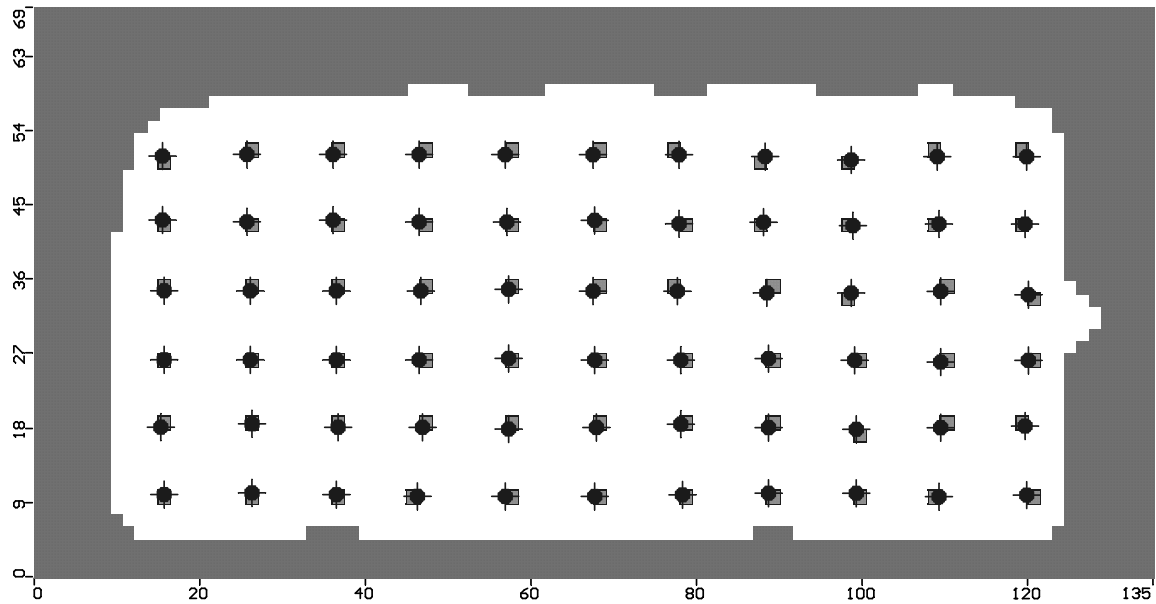


Figure 4-4 Extraction Wells Viewed from Top

Model Calibration

Once all of the input parameters are entered into MODFLOW and the model is run, heads are generated at points in space within the wetland. These modeled heads can be compared to the heads that were measured using the piezometers in the field. Since the calculated heads did not initially match the measured heads, the model had to be calibrated. The two parameters that can be adjusted for model calibration are the middle layer conductivity value and the constant head value at the weir. Using a middle layer conductivity of 0.00004 ft/s and a constant head value of 4.7 ft, the calculated head best matched the measured head, as seen in Figure 4-5.

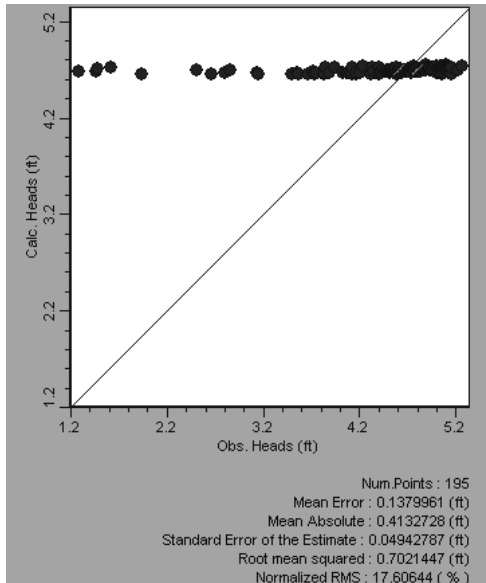


Figure 4-5 Calculated Vs. Observed Head

Ideally, calculated and observed data would coincide, and the points in Figure 4-5 would fall along the diagonal line in the graph. Obviously, this is not the case for the current analysis. In his thesis, Entingh (2002) calibrated his model by adjusting hydraulic conductivities around the coordinate locations of the piezometers within the model until the calculated heads matched the actual heads. The conductivities were not adjusted in this study since more confidence is placed in the values obtained with the pump tests, using the 2-inch diameter observation wells that were not available to Entingh. Instead, the constant head and middle-layer conductivity were adjusted until the average of the measured head values were on the diagonal line of Figure 4-5. The outliers to the left of the

diagonal line are all piezometers that were in the bottom layer. The observed values are lower than the calculated values most likely due to the fact that some of the well screens may have been at or below the liner.

Model Output

There are many aspects to the output of a MODFLOW model. For this thesis, the focus will be on the potentiometric surface in each layer, the direction and rate of flow, and the path taken by water molecules as they enter the wetland to help generate a residence time distribution function (RTDF). From this analysis, we will attempt to describe and understand the groundwater flow in the wetland.

Potentiometric Surface

The potentiometric surface simulated using MODFLOW can be represented by use of the two-dimensional equipotential contour map. MODFLOW provides an equipotential contour map for each layer of the wetland. Figure 4-6 is an example of such a map in the first soil layer of the wetland looking down from the top. Figure 4-7 and 4-8 are elevation views showing the equipotential heads along the length and width of the wetland. Each elevation view slice was taken from the midsection of the wetland. Other contour maps for each layer can be found in Appendix D.

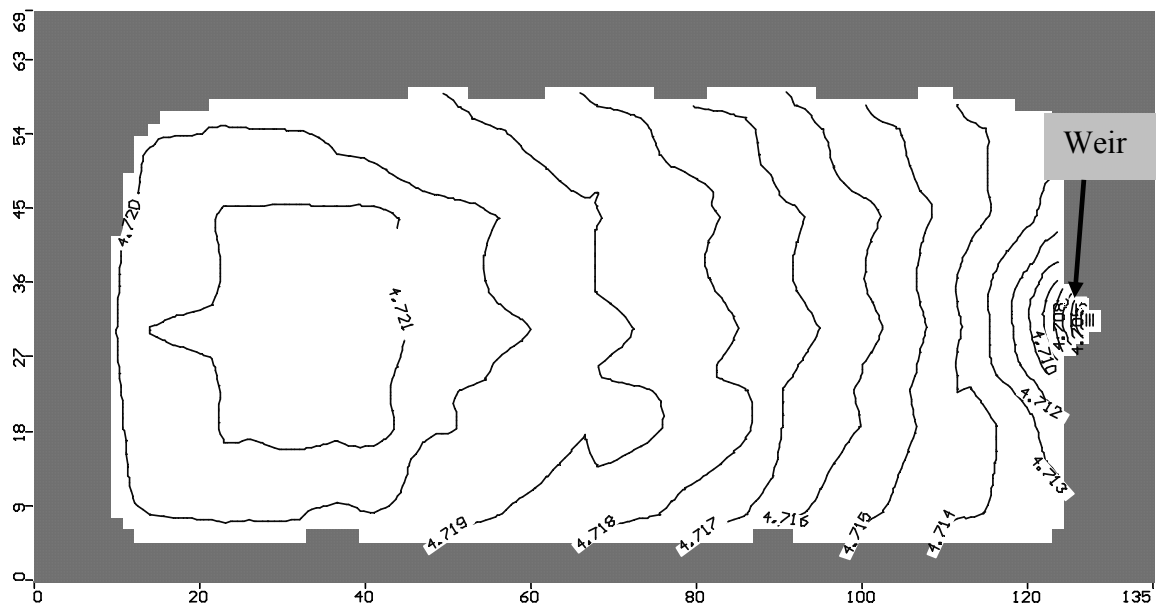


Figure 4-6 Contours of Equipotential Head of Layer 1 from the Top

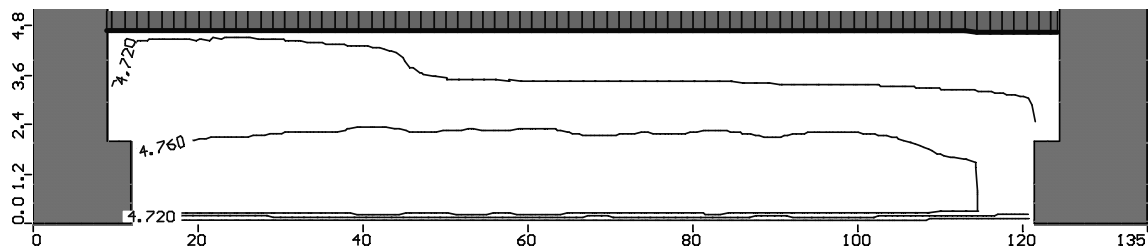


Figure 4-7 Lengthwise Elevation Profile Along the Mid-section of the Wetland Showing Equipotential Head Contours

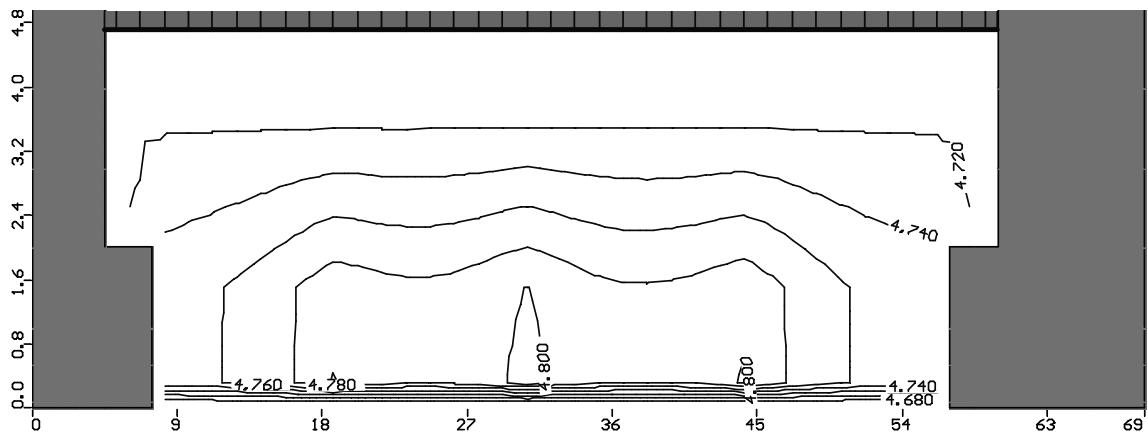


Figure 4-8 Widthwise Elevation Profile along the Midsection of the Wetland Showing Equipotential Head Contours

The two-dimensional views only provide a slice out of the wetland. A better view would be in three dimensions, providing an equipotential surface for a 2-D layer. MODFLOW has the ability to export the equipotential head data to a file with the x and y coordinates and the head value. These three components can be graphed in Surfer 8.0 to provide the equipotential surface for each layer. The surface plot for the first soil layer is in Figure 4-9. The rest of the surface plots of each layer are in Appendix D, matched with their 2-D contour plots.

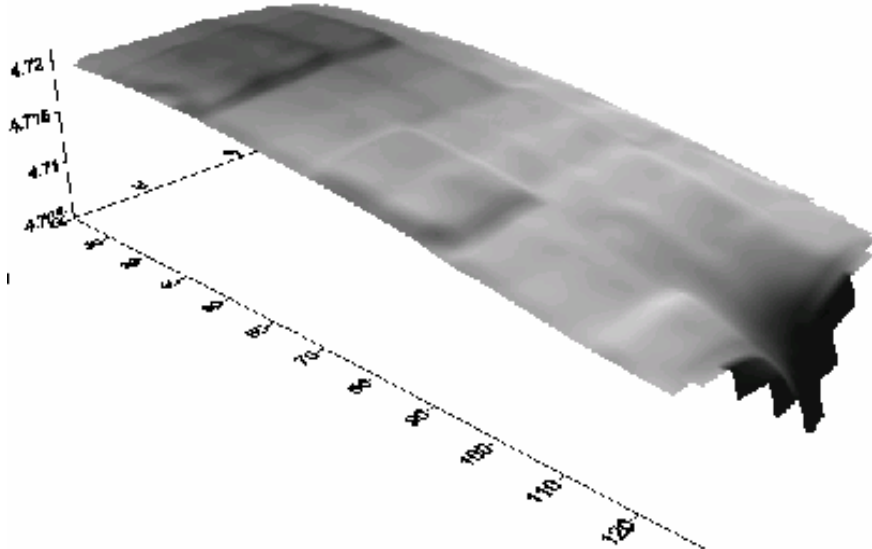


Figure 4-9 Equipotential Head Surface Plot for Top Layer

The weir end of the 3-D image is on the right side. This image indicates that the head measurement is low at the weir and high at the inlet end, as would be expected.

Flow Visualization

The direction of flow is different throughout the wetland.

MODFLOW has a function that places arrows in the direction of flow at specified points in space. Figure 4-10 gives an example of the general direction of flow by viewing an elevation view along the midsection of the wetland model.

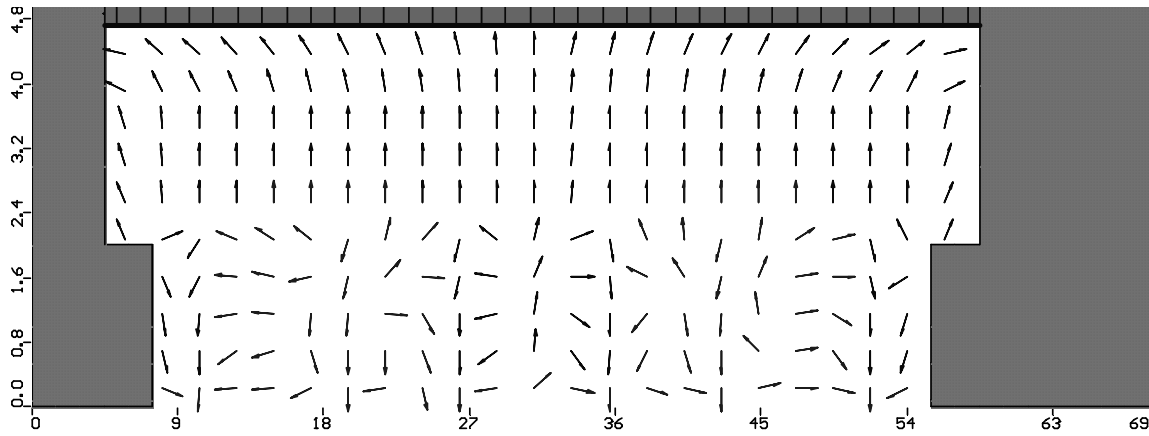


Figure 4-10 Elevation View Showing Flow Directions

The water moves upward above the inlet pipes and back down the sides of the wetland and between the pipes due to the leakage occurring. In Appendix E are cross-sections at various locations throughout the wetland. These provide the reader with a clear idea of where the water is going.

The direction of flow is important to give a general idea of the dynamics of the wetland, but note that the arrows only indicate direction, not speed. MODFLOW has the capability to calculate and export velocity data for the wetland. The program provides an x, y, and z initial

coordinate, followed by the velocity component in the x-, y-, and z-directions. The equation for the velocity vector with all three components is

$$\mathbf{v} = v_x \mathbf{i} + v_y \mathbf{j} + v_z \mathbf{k} \quad (27)$$

The magnitude of the velocity at any given point is

$$s = \sqrt{v_x^2 + v_y^2 + v_z^2} \quad (28)$$

where s is the speed of the water molecule.

Path Lines and Residence Times

The velocity of water molecules explains a lot about the dynamics of the flow within the wetland. However, as a water molecule travels through the wetland, it may be hard to visualize the path that the molecule will take by only looking at the velocity at points in space. Visual MODFLOW contains additional software called MODPATH that provides the capability of showing the path of a molecule over time as it travels from a specified starting position. In addition to its path, arrows are placed along the path at set time increments so that one can get an idea of the speed of the molecule.

To illustrate the paths that molecules take, 5 molecules were chosen at random places in the wetland. Figure 4-11 shows a top view of the 5 molecules chosen. Molecules A and B are in the second soil layer, and

molecules C, D, and E are in the third soil layer. No molecules were chosen from the top layer of soil since they all went to the weir. No molecules were chosen from the gravel layer since the majority of those molecules exited through the bottom of the wetland. As can be seen with the molecules in the third layer of soil, one molecule went to the weir while two leaked out of the wetland. The location of the exit of molecules D and E are under piezometers 52C and 60C respectively.

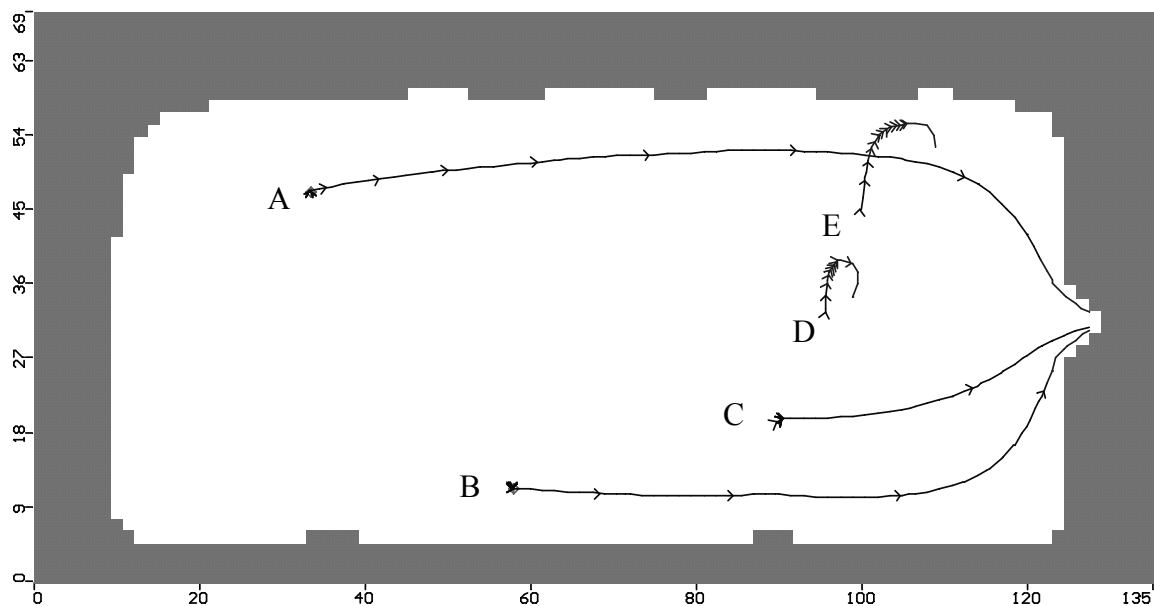


Figure 4-11 View of Paths of Selected Molecules

To get a better idea of the actual paths taken by the molecules, an elevation view along the length and width of the wetland are provided in Figure 4-12 and 4-13.

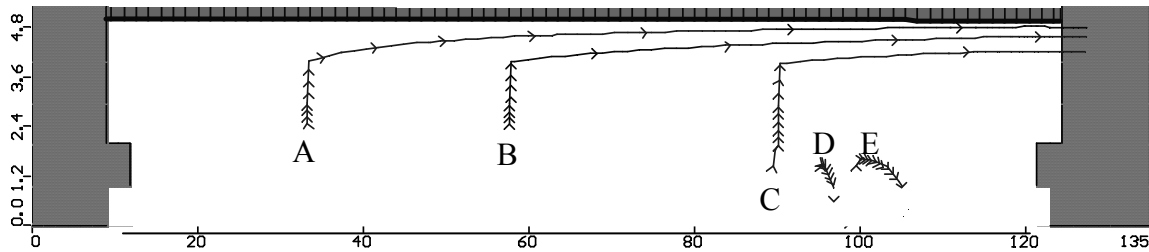


Figure 4-12 Elevation Profile of Molecule Paths

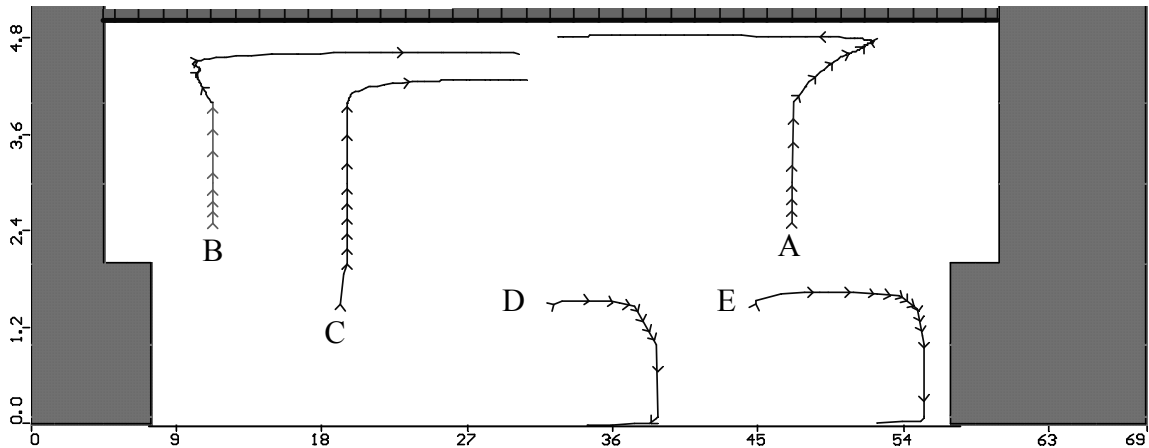


Figure 4-13 Width Elevation Profile of Molecule Paths

The time increment between the arrowheads on the path lines is 0.1 day. This gives the following information for residence times:

Table 4-4 Residence Times

Particle	Approximate Residence Time (Days)
A	1.5
B	1.3
C	1.2
D	0.9
E	1.3

By observing the proximity of the heads of arrows, one can deduce the velocity of the molecule. Heads close together would indicate a low velocity.

The coordinates of each molecule's location as it travels through the wetland can be exported from MODFLOW. The data for each coordinate along the path of the five molecules shown in Figures 4-11 through 4-13 can be found in Appendix F. The coordinates of the data points are given as the center of the path as it passes through the individual cells within the wetland model. Each cell is 1.5 feet x 1.5 feet x layer thickness (1 foot in the case of the top, middle, and bottom soil layers).

Residence Time Distribution Function (RTDF)

Using the methods discussed at the end of chapter 3, the cumulative RTDF, $F(t)$, was constructed and shown in Figure 4-14.

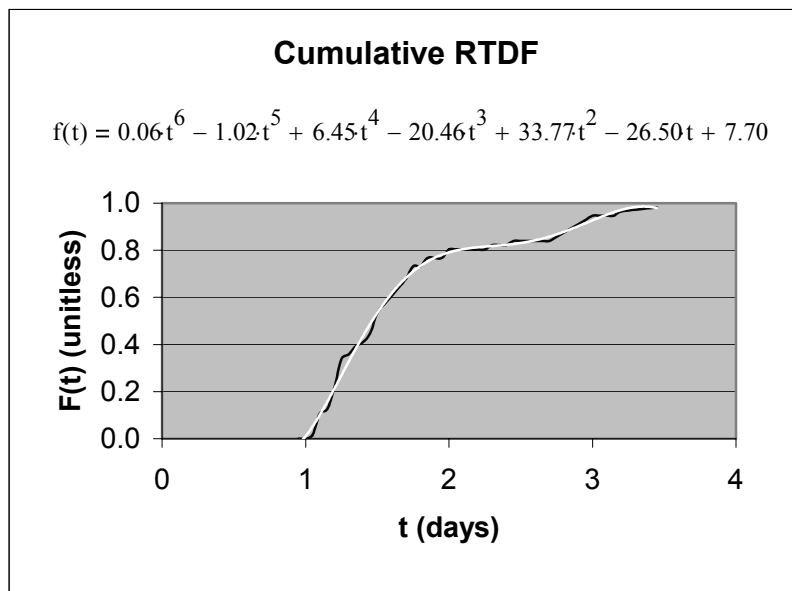


Figure 4-14 Cumulative RTDF

The dark line in the picture is the line resulting from graphing the $F(t)$ data versus time. The white line is the trend line for the data generated by Excel. The equation on the chart is a 6th order polynomial that fit the $F(t)$ data. The $F(t)$ data that were graphed are tabulated in Appendix G.

The derivative of the equation on the graph in Figure 4-14 was calculated and graphed as $f(t)$, shown in Figure 4-15.

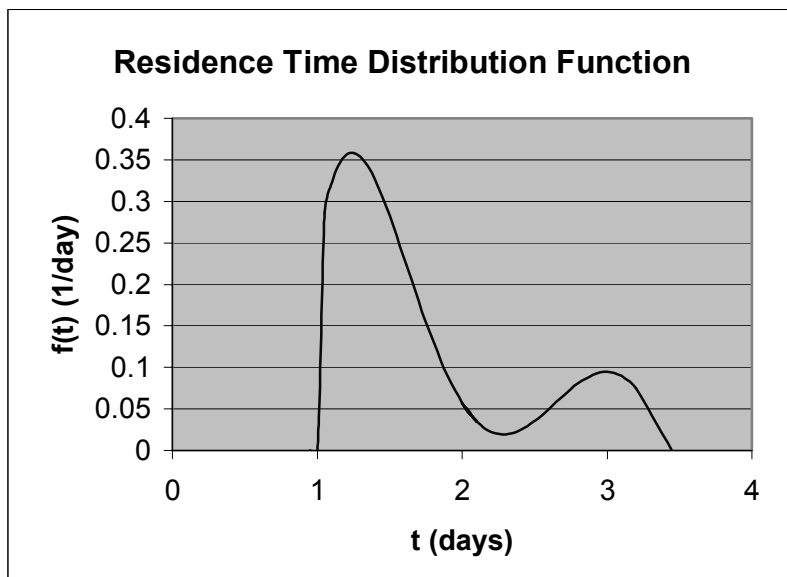


Figure 4-15 RTDF

The equation for the graph in Figure 4-15 is

$$f(t) = 0.38t^5 - 5.10t^4 + 25.81t^3 - 61.38t^2 + 67.55t - 26.50 \quad (29)$$

The RTDF does not exactly resemble Figure 2-4, but appears instead to be bi-modal. This indicates that at some point during the transport of water molecules, the number of molecules exiting the weir slowed, then increased once more. There may be several explanations for this phenomenon. One reason for the bi-modal shape could be due to the multi-directional flow paths caused by leakage (see Figure 4-10). As the molecules start in an upward direction, some may be diverted sideways before continuing upward, delaying their arrival at the outlet. Another possible reason for the bi-modal shape is due to the hydraulic conductivities assigned to the model. If some of the regions (see Figure 4-4) have lower conductivities than regions surrounding them, flow through the high conductivity regions may result in early breakthrough of some fraction of the flow, while the remainder of the flow will reach the outlet at a later time.

Mean Residence Time

The mean residence time was calculated by inserting the $f(t)$ equation 29 into equation 26.

$$\tau = \int_0^{\infty} f(t) \cdot t \, dt \quad (26)$$

The result is a residence time of 1.6 days.

The calculated mean residence time may be compared to the theoretical mean residence time, V/Q . For this calculation, the volume in question is the volume of pore water in the wetland that is swept by water that flows out the weir. Since only $1/3$ of the water is going out the weir, then $1/3$ of the total pore volume should be used in the calculation. The total volume of the wetland is 172,000 Gallons. The pore volume of the wetland is the total volume multiplied by the average porosity, 0.27. This gives a total pore volume of 46,600 Gal. Since $1/3$ of the influent flow goes out the weir, we'll assume that this fraction of the influent flows through a volume that is $1/3$ of the total pore volume, or 15,518 Gal. The flow, Q , used to calculate the theoretical mean residence time should be $1/3$ of the total flow. Since the total flow into the wetland is 15 GPM, the flow going out the weir is 5 GPM. The theoretical mean residence time is then 15,518 Gal / 5 GPM = 3,104 minutes, or 2.16 days.

For a given pore volume and flow rate, the theoretical mean residence time is the "best" (i.e. longest) residence time possible. If the actual residence time in a system is equal to the theoretical residence time, it indicates that the flow is evenly distributed throughout the system. Since the numerical model of the wetland in this study has

a mean residence time less than theoretical, it indicates that the model is simulating regions of stagnant water in the wetland. That is, there are fractions of the wetland volume that are modeled as not being swept by flow, so the mean residence time calculated using water molecules exiting the weir is less than the theoretical residence time which was calculated based on flow and pore volume. Knowing this, the residence time, and therefore extent of contaminant destruction, can be increased by focusing on ways to reduce the fraction of stagnant zones.

V. Conclusions and Recommendations for Further Study

The purpose of the constructed treatment wetland investigated in this study is to biodegrade contaminated groundwater. The flow of the groundwater through the wetland should ideally be vertical, without stagnation or shortcircuiting occurring. In this study, the flow of water through wetland cell 2 at Wright-Patterson Air Force Base was analyzed in order to develop a better understanding of actual flow paths, and how deviations from ideal flow might affect degradation efficiency. The results of this study provide some understanding about how water flows through the constructed wetland.

Since the liner under the wetland was penetrated multiple times during construction, the flow dynamics were considerably different than designed. With 2/3 of the inflow leaking out the bottom of the wetland, the majority of flow in the bottom layers leaked out. Most of the water that made it into the upper wetland layers generally traveled on to the weir. Clearly, the flow is not uniformly vertical as designed. The difference between the calculated and theoretical mean residence time indicates that even the flow that does travel to the weir is not

uniformly vertical, and there are stagnant zones in the wetland.

From viewing the three-dimensional graphs of head contours in Appendix D, the highest heads are found directly above the inflow pipes, as expected. Between the pipes, however, the head is lower, causing water to flow toward the bottom of the wetland.

The analysis of the effect on wetland flow with various loading rates was not attempted due to the shutdown of the wetland. The flow could not be increased much more because the bentonite seal around the piezometers might not be able to withstand much more pressure.

The RTDF calculated in this thesis provides useful information in characterizing the flow. The RTDF plot was bi-modal, indicating that a delay of molecules exiting the weir takes place most likely due to multi-directional flow due to leakage or varying hydraulic conductivities.

Study Strengths

A wetland model was built using MODFLOW that attempted to simulate the real-world situation by taking into account the leakage that was discovered in the liner. The methods used in building the model can be applied to other wetland studies. Also, the head and hydraulic conductivity data

that were gathered could be further analyzed in other studies. The particle tracing capability of the MODFLOW software provided a good representation of the possible paths followed by water molecules. This can be verified with a tracer test.

The RTDF is a useful tool for studies of reactions within wetlands. The method for developing the RTDF can be applied to a constructed wetland that does not leak in order to obtain valuable flow information for predicting degradation efficiency.

Study Weaknesses

The obvious weakness to this study is due to the unexpected penetration of the liner. The original goal of checking for vertical flow was affected since a lot of the water was leaking back into the ground. The comparison of this thesis to Entingh's (2002) thesis is not possible because of the holes in the liner. With the exact location of the liner unknown, the exact location of the bottom-layer piezometers relative to the liner could not be determined. The screens could have been above, below, or somewhere in between the liner. Since the upper two layers of piezometers were not in their presumed layer, there was no data for the second soil layer. There is no accurate

way to test if the estimated hydraulic conductivity used was correct. Using the second soil layer as a fitting parameter for the model did not give a better fit to the measured vs. calculated head data. Last, the method for measuring hydraulic conductivities was a good choice; however, more than 6 data points would help verify the values of conductivities that were obtained.

Recommendations for Further Study

- (1) Take velocity and soil parameter data from the model and analyze it to determine the effect of the soil on the velocity of the flow in the wetland.
- (2) Reroute the flow of water to above the wetland cell and analyze it as a surface-flow treatment wetland, using the three layers of piezometers as monitors for flow and contamination samples.
- (3) Use the model methods developed for this wetland and apply them to another constructed treatment wetland. Test the residence time distribution function method by applying a dye-tracer test.
- (4) Couple the RTDF with reaction kinetics to predict effluent concentrations.
- (5) Experiment with more varieties of soil and flow rates in similar constructed treatment wetlands. Try maximizing

the residence time efficiency with a more evenly distributed vertical flow.

Appendix A: Piezometer Data

Nest	Local Coordinates (ft)			Elevation of Coupling (ft)	Elevation of Screen (ft)	Average Water Level (ft)	Head (ft)
	X	Y	Z				
1	A	15.940	11.016	4.442	3.192	0.370	4.812
	B	15.000	10.000	3.940	1.690	1.118	5.058
	C	15.791	9.943	4.500	0.250	-0.300	4.200
2	A	15.661	19.105	4.499	3.249	0.205	4.704
	B	14.491	18.290	4.001	1.751	1.035	5.035
	C	15.482	18.146	4.564	0.314	-0.363	4.201
3	A	15.686	27.462	4.336	3.086	0.639	4.975
	B	14.926	26.380	4.135	1.885	0.976	5.110
	C	15.745	26.346	4.562	0.312	-0.363	4.200
4	A	15.859	35.473	4.590	3.340	0.406	4.996
	B	14.924	34.813	4.162	1.912	0.983	5.144
	C	15.794	34.682	4.623	0.373	0.462	5.085
5	A	15.481	44.149	4.378	3.128	0.521	4.899
	B	14.448	43.137	4.037	1.787	0.753	4.790
	C	15.579	43.188	4.512	0.262	-0.925	3.587
6	A	15.519	51.904	4.287	3.037	0.476	4.763
	B	14.470	50.778	3.993	1.743	0.833	4.826
	C	15.529	50.874	4.546	0.296	-1.025	3.521
7	A	26.256	11.045	4.567	3.317	0.392	4.959
	B	25.241	10.092	4.282	2.032	0.844	5.125
	C	26.332	10.113	4.485	0.235	-0.338	4.148
8	A	26.143	18.999	4.029	2.779	0.776	4.805
	B	25.206	18.019	4.185	1.935	0.944	5.129
	C	26.025	17.922	4.574	0.324	-0.125	4.449
9	A	26.336	27.326	4.462	3.212	0.382	4.844
	B	25.196	26.291	4.186	1.936	0.934	5.120
	C	26.194	26.356	4.502	0.252	-0.438	4.064
10	A	26.139	35.720	4.456	3.206	0.267	4.723
	B	25.083	34.716	4.177	1.927	0.896	5.072
	C	26.186	34.610	4.668	0.418	-0.800	3.868
11	A	25.871	44.076	4.442	3.192	0.031	4.473
	B	25.042	42.832	4.267	2.017	0.826	5.093
	C	25.889	42.913	4.653	0.403	-0.900	3.753

Nest	Local Coordinates (ft)			Elevation of Coupling (ft)	Elevation of Screen (ft)	Average Water Level (ft)	Head (ft)
	X	Y	Z				
12	A	25.652	52.077	4.438	3.188	0.191	4.629
	B	24.777	51.086	4.231	1.981	0.552	4.783
	C	25.754	51.229	4.762	0.512	-1.163	3.599
13	A	36.736	10.931	4.526	3.276	0.056	4.582
	B	35.660	10.074	4.328	2.078	0.816	5.144
	C	36.604	10.033	4.741	0.491	-0.975	3.766
14	A	36.547	19.258	4.548	3.298	0.253	4.801
	B	35.681	18.177	4.307	2.057	0.813	5.120
	C	36.722	18.222	4.699	0.449	-0.500	4.199
15	A	36.483	27.422	4.458	3.208	0.122	4.580
	B	35.684	26.413	4.241	1.991	0.677	4.918
	C	36.507	26.324	4.615	0.365	0.153	4.768
16	A	36.574	35.711	4.654	3.404	0.000	4.654
	B	35.568	34.543	4.440	2.190	0.681	5.120
	C	36.510	34.695	4.712	0.462	-0.600	4.112
17	A	36.255	44.396	4.752	3.502	-0.075	4.677
	B	35.275	43.287	4.339	2.089	0.785	5.123
	C	36.211	43.245	4.557	0.307	0.479	5.036
18	A	36.122	52.097	4.581	3.331	0.330	4.911
	B	35.147	51.145	4.341	2.091	0.750	5.091
	C	36.101	51.239	4.645	0.395	-0.725	3.920
19	A	46.984	10.758	4.654	3.404	0.024	4.678
	B	45.285	9.736	4.195	1.945	0.896	5.090
	C	46.422	9.782	4.643	0.393	-0.950	3.693
20	A	46.952	19.043	4.731	3.481	0.066	4.797
	B	46.102	18.055	4.392	2.142	0.719	5.110
	C	47.019	18.030	4.836	0.586	-0.575	4.261
21	A	46.688	27.148	4.698	3.448	-0.100	4.598
	B	45.796	26.174	4.315	2.065	0.797	5.112
	C	46.680	26.232	4.907	0.657	-0.750	4.157
22	A	46.977	35.601	4.527	3.277	0.021	4.548
	B	45.789	34.474	4.334	2.084	0.823	5.157
	C	46.877	34.633	4.628	0.378	-0.525	4.103

Nest	Local Coordinates (ft)			Elevation of Coupling (ft)	Elevation of Screen (ft)	Average Water Level (ft)	Head (ft)
	X	Y	Z				
23	A	46.673	43.991	4.692	3.442	-0.175	4.517
	B	45.658	42.830	4.274	2.024	0.833	5.107
	C	46.683	42.988	4.610	0.360	-0.375	4.235
24	A	46.404	52.089	4.117	2.867	0.628	4.745
	B	45.303	51.252	4.125	1.875	1.007	5.132
	C	46.513	51.206	4.428	0.178	-0.650	3.778
25	A	57.516	10.845	4.552	3.302	0.087	4.639
	B	56.017	9.808	4.449	2.199	0.701	5.150
	C	57.049	9.776	4.733	0.483	-0.125	4.608
26	A	57.539	18.862	4.634	3.384	0.101	4.735
	B	56.487	18.050	4.401	2.151	0.747	5.147
	C	57.480	18.012	4.628	0.378	-0.875	3.753
27	A	57.479	27.302	4.801	3.551	0.010	4.811
	B	56.329	26.472	4.418	2.168	0.774	5.192
	C	57.368	26.404	4.760	0.510	-0.650	4.110
28	A	57.449	35.577	4.774	3.524	-0.200	4.574
	B	56.409	34.673	4.513	2.263	0.483	4.995
	C	57.350	34.756	4.765	0.515	-0.625	4.140
29	A	57.214	43.987	4.762	3.512	-0.200	4.562
	B	56.113	43.023	4.489	2.239	0.667	5.155
	C	57.195	43.059	4.666	0.416	-0.525	4.141
30	A	57.085	51.635	4.023	2.773	0.729	4.752
	B	56.074	50.942	3.854	1.604	1.444	5.298
	C	57.090	51.124	4.307	0.057	-	-
31	A	68.195	10.898	4.661	3.411	0.073	4.734
	B	66.710	9.787	4.256	2.006	0.885	5.141
	C	67.718	9.836	4.756	0.506	-0.900	3.856
32	A	68.074	18.905	4.614	3.364	0.042	4.656
	B	67.185	18.055	4.381	2.131	0.809	5.190
	C	68.040	18.041	4.779	0.529	-0.400	4.379
33	A	67.794	27.210	4.631	3.381	0.056	4.687
	B	66.814	26.199	4.380	2.130	0.795	5.175
	C	67.754	26.273	4.893	0.643	0.297	5.190

Nest	Local Coordinates (ft)			Elevation of Coupling (ft)	Elevation of Screen (ft)	Average Water Level (ft)	Head (ft)
	X	Y	Z				
34	A	67.800	35.430	4.362	3.112	0.292	4.654
	B	66.678	34.551	4.426	2.176	0.722	5.148
	C	67.649	34.559	4.750	0.500	-0.075	4.675
35	A	67.818	44.209	4.404	3.154	0.229	4.633
	B	66.764	42.975	4.320	2.070	0.813	5.132
	C	67.832	43.219	4.819	0.569	-0.850	3.969
36	A	67.673	51.809	4.247	2.997	0.635	4.882
	B	66.872	51.274	4.272	2.022	0.615	4.886
	C	67.696	51.146	4.778	0.528	-1.600	3.178
37	A	78.547	10.975	4.844	3.594	-0.100	4.744
	B	77.244	9.821	4.515	2.265	0.622	5.136
	C	78.382	9.968	4.678	0.428	-0.250	4.428
38	A	78.279	19.369	4.555	3.305	0.014	4.569
	B	77.258	18.363	4.456	2.206	0.684	5.140
	C	78.189	18.439	4.712	0.462	-1.875	2.837
39	A	78.364	27.219	4.591	3.341	-0.075	4.516
	B	77.167	26.363	4.311	2.061	0.785	5.095
	C	78.306	26.348	4.586	0.336	-1.425	3.161
40	A	78.042	35.666	4.438	3.188	0.118	4.556
	B	76.836	34.706	4.468	2.218	0.625	5.093
	C	77.881	34.568	4.615	0.365	-0.375	4.240
41	A	78.008	43.956	4.746	3.496	-0.200	4.546
	B	77.042	42.863	4.338	2.088	0.757	5.095
	C	78.008	42.892	4.850	0.600	0.115	4.965
42	A	77.996	52.161	4.490	3.240	0.208	4.698
	B	77.015	51.004	4.132	1.882	0.854	4.986
	C	77.923	51.192	4.398	0.148	0.781	5.179
43	A	88.965	11.077	4.616	3.366	0.049	4.665
	B	87.957	10.102	4.281	2.031	0.734	5.015
	C	88.881	10.097	4.643	0.393	-1.950	2.693
44	A	88.827	18.980	4.703	3.453	-0.100	4.603
	B	88.030	18.031	4.356	2.106	0.757	5.113
	C	88.866	18.021	4.734	0.484	0.075	4.809

Nest	Local Coordinates (ft)			Elevation of Coupling (ft)	Elevation of Screen (ft)	Average Water Level (ft)	Head (ft)
	X	Y	Z				
45	A	88.736	27.360	4.628	3.378	-0.125	4.503
	B	87.743	26.396	4.338	2.088	0.778	5.115
	C	88.711	26.445	4.830	0.580	-0.950	3.880
46	A	88.595	35.341	4.570	3.320	0.024	4.594
	B	87.623	34.590	4.537	2.287	0.608	5.144
	C	88.603	34.517	4.835	0.585	-0.475	4.360
47	A	88.426	43.874	4.882	3.632	-0.300	4.582
	B	87.300	42.910	4.350	2.100	0.760	5.110
	C	88.288	42.923	4.774	0.524	-0.225	4.549
48	A	88.391	51.927	4.576	3.326	0.115	4.691
	B	87.397	50.947	4.096	1.846	0.792	4.887
	C	88.345	50.984	4.695	0.445	-2.725	1.970
49	A	99.495	11.137	4.349	3.099	0.288	4.637
	B	98.547	10.028	4.258	2.008	0.868	5.126
	C	99.406	10.114	4.635	0.385	-	-
50	A	99.337	18.851	4.765	3.515	-0.175	4.590
	B	98.254	17.909	4.264	2.014	0.865	5.128
	C	99.330	17.949	4.711	0.461	-0.250	4.461
51	A	99.251	27.293	4.650	3.400	-0.100	4.550
	B	98.203	26.153	4.361	2.111	0.580	4.941
	C	99.180	26.178	4.812	0.562	-0.375	4.437
52	A	98.921	35.451	4.830	3.580	-0.325	4.505
	B	98.020	34.266	4.354	2.104	0.266	4.619
	C	98.864	34.437	4.731	0.481	0.391	5.122
53	A	98.999	43.586	4.907	3.657	-0.300	4.607
	B	98.185	42.458	4.327	2.077	0.778	5.104
	C	98.983	42.581	4.656	0.406	0.406	5.062
54	A	98.980	51.580	4.486	3.236	0.264	4.750
	B	97.940	50.611	4.023	1.773	0.976	4.998
	C	98.797	50.644	4.531	0.281	0.552	5.083
55	A	109.977	10.672	4.906	3.656	-0.150	4.756
	B	108.152	9.627	4.508	2.258	0.625	5.133
	C	109.326	9.738	4.835	0.585	-3.525	1.310

Nest	Local Coordinates (ft)			Elevation of Coupling (ft)	Elevation of Screen (ft)	Average Water Level (ft)	Head (ft)
	X	Y	Z				
56	A	109.679	19.145	4.818	3.568	-0.200	4.618
	B	108.749	18.042	4.573	2.323	0.208	4.781
	C	109.625	18.100	4.849	0.599	-3.200	1.649
57	A	109.722	27.105	5.038	3.788	-0.400	4.638
	B	108.649	26.100	4.560	2.310	0.101	4.660
	C	109.610	26.140	4.902	0.652	-0.325	4.577
58	A	109.691	35.569	4.908	3.658	-0.200	4.708
	B	108.673	34.520	4.605	2.355	0.141	4.745
	C	109.655	34.572	4.910	0.660	0.042	4.952
59	A	109.698	43.557	4.750	3.500	-0.100	4.650
	B	108.462	42.802	4.528	2.278	0.344	4.871
	C	109.361	42.737	4.902	0.652	0.150	5.052
60	A	109.289	51.967	4.423	3.173	0.247	4.670
	B	108.331	51.081	4.197	1.947	0.854	5.051
	C	109.291	51.050	4.569	0.319	-0.219	4.350
61	A	120.210	11.005	4.738	3.488	0.128	4.866
	B	119.197	10.000	4.327	2.077	0.934	5.261
	C	120.058	9.907	4.808	0.558	-	-
62	A	119.878	19.343	4.926	3.676	-0.125	4.801
	B	118.963	17.789	4.435	2.185	0.448	4.883
	C	119.850	18.405	4.906	0.656	-3.400	1.506
63	A	120.479	27.248	5.063	3.813	-0.325	4.738
	B	119.467	26.278	4.578	2.328	0.323	4.901
	C	120.298	26.272	4.939	0.689	-2.400	2.539
64	A	120.262	35.305	4.960	3.710	-0.200	4.760
	B	119.460	34.333	4.505	2.255	0.573	5.078
	C	120.235	34.316	4.994	0.744	-2.100	2.894
65	A	119.758	43.820	4.892	3.642	-0.150	4.742
	B	118.947	42.669	4.437	2.187	0.493	4.930
	C	119.738	42.881	4.875	0.625	0.063	4.938
66	A	119.821	51.889	4.833	3.583	0.000	4.833
	B	118.956	50.890	4.489	2.239	0.434	4.923
	C	119.939	51.044	4.849	0.599	-3.350	1.499

***Local coordinates based on the corner of the wetland closest to the pumphouse.**

***Elevations based on an estimated location of the liner being 4.5 feet under the coupling on Piezometer 1C.**

***No water was found in 30C, 49C, and 61C.**

Appendix B: Porosity Data

Depth (cm)	Volume (cm ³)	Wet Weight (g)	Drained Weight (g)	Specific Yield	Dry Weight (g)	Porosity	Specific Storage (ft ⁻¹)
0-10	20.80	42.42	41.39	0.05	30.24	0.29	0.00039084
10-20	24.39	35.30	33.92	0.06	25.62	0.27	0.00039082
20-30	13.82	30.79	29.98	0.06	22.77	0.26	0.00039080
30-40	13.82	34.41	33.27	0.08	23.87	0.31	0.00039087
40-50	15.63	54.62	53.20	0.09	47.37	0.13	0.00039062
50-60	9.26	21.04	19.51	0.17	15.77	0.25	0.00039079
60-70	No Sample	-	-	-	-	-	-
70-80	8.00	20.44	18.88	0.20	15.10	0.26	0.00039080
80-90	17.58	29.48	28.28	0.07	22.46	0.24	0.00039077
90-120				0.25		0.30	0.00025030

*Core Sample taken between Piezometers 46 and 52.
 *90-120 cm values estimated by assuming sand/gravel below 90 cm

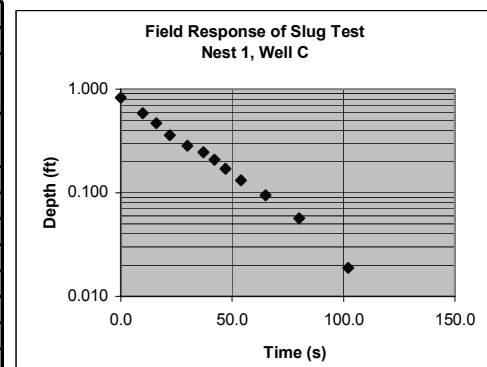
There were three measurements taken from each soil layer, every 10 centimeters. With each of the three soil layers being one foot (30 centimeters) thick, the first 3 rows of the table in Appendix B are the top layer, followed by the next 3 rows being the middle layer, and finally the rows from 60-90 centimeters being the bottom layer. Beyond 90 centimeters is the gravel layer for which the values of porosity and specific yield were estimated from tables in the book "Physical and Chemical Hydrology" by Domenico and Schwartz (Domenico & Schwartz, 1998:14,68). For each individual soil layer, the three values of specific yield and porosity were averaged (Table 4-1) so that the calculated property was the same throughout the layer.

Appendix C: Slug Test Data

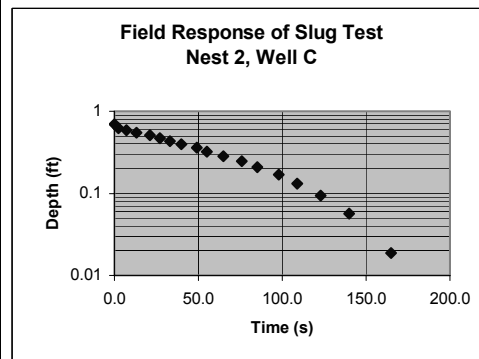
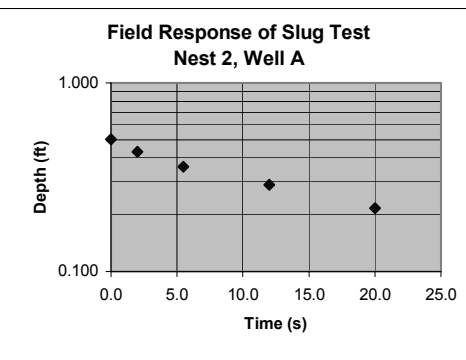
Nest 1 (Between Piezometers 7 and 8)				
A				
Slug Size	1/2 L slug			
Initial Depth, h_o (ft)	1.00			
Time (s)	Dist from top (ft)	Depth, h (ft)	h/h_o	
0.0	0.583	0.417	0.417	
2.5	0.792	0.208	0.208	
6.7	0.958	0.042	0.042	
10.9	1.000	0.000	0.000	

B				
1 L slug				
Initial Depth, h_o (ft)	2.10			
Time (s)	Dist from top (ft)	Depth, h (ft)	h/h_o	
0.0	1.500	0.600	0.286	
2.5	1.700	0.400	0.190	
6.0	2.000	0.100	0.048	
9.0	2.100	0.000	0.000	

C				
2 L slug				
Initial Depth, h_o (ft)	2.65			
Time (s)	Dist from top (ft)	Depth, h (ft)	h/h_o	
0.0	0.458	2.192	0.827	
10.0	1.100	1.550	0.585	
16.0	1.400	1.250	0.472	
22.0	1.700	0.950	0.358	
30.0	1.900	0.750	0.283	
37.0	2.000	0.650	0.245	
42.0	2.100	0.550	0.208	
47.0	2.200	0.450	0.170	
54.0	2.300	0.350	0.132	
65.0	2.400	0.250	0.094	
80.0	2.500	0.150	0.057	
102.0	2.600	0.050	0.019	
144.0	2.650	0.000	0.000	

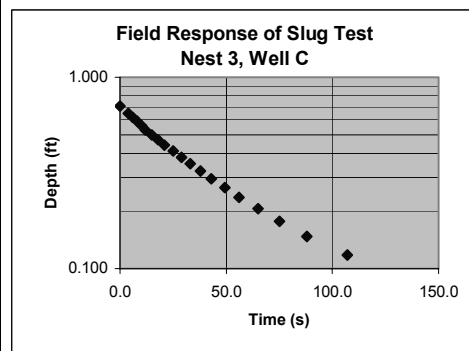
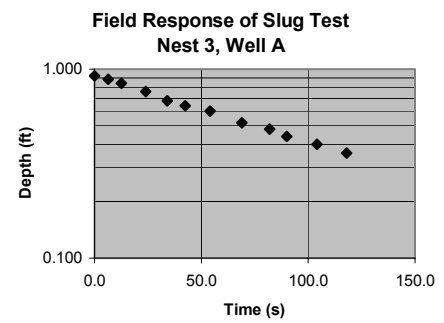


Nest 2 (Between Piezometers 17 and 18)								
Slug Size	A			B				
	1/2 L slug							
Initial Depth, h_o (ft)	1.17			2.10				
	Time (s)	Dist from top (ft)	Depth, h (ft)	h/h _o	Time (s)			
	0.0	0.583	0.587	0.501	0.0	1.500	0.600	0.286
	2.0	0.667	0.503	0.430	2.5	2.090	0.010	0.005
	5.5	0.750	0.420	0.359				
	12.0	0.833	0.337	0.288				
	20.0	0.917	0.253	0.217				
	28.0	1.000	0.170	0.145				
C								
Slug Size	2 L slug							
Initial Depth, h_o (ft)	2.65							
	Time (s)	Dist from top (ft)	Depth, h (ft)	h/h _o				
	0.0	0.800	1.850	0.698				
	2.5	1.000	1.650	0.623				
	7.0	1.100	1.550	0.585				
	13.0	1.200	1.450	0.547				
	21.0	1.300	1.350	0.509				
	27.0	1.400	1.250	0.472				
	33.0	1.500	1.150	0.434				
	40.0	1.600	1.050	0.396				
	49.0	1.700	0.950	0.358				
	55.0	1.800	0.850	0.321				
	65.0	1.900	0.750	0.283				
	76.0	2.000	0.650	0.245				
	85.0	2.100	0.550	0.208				
	98.0	2.200	0.450	0.170				
	109.0	2.300	0.350	0.132				
	123.0	2.400	0.250	0.094				
	140.0	2.500	0.150	0.057				
	165.0	2.600	0.050	0.019				
	215.0	2.650	0.000	0.000				



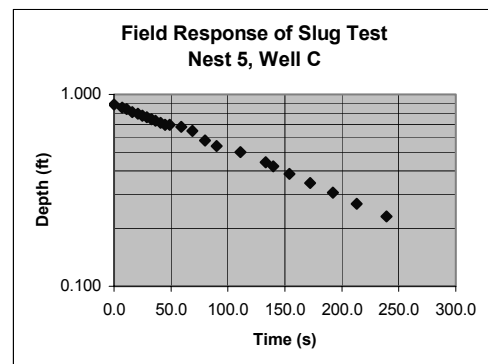
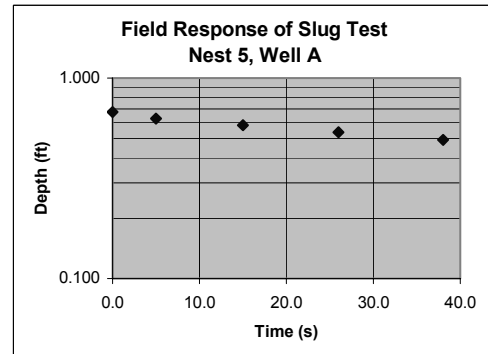
Well 3 (Between Piezometers 34 and 35)				
Slug Size Initial Depth, h_o (ft)	A		B	
	0.7 L slug		1 L slug	
	1.04		2.15	
Time (s)	Dist from top (ft)	Depth, h (ft)	h/h _o	
0.0	0.083	0.958	0.920	
6.5	0.125	0.917	0.880	
12.5	0.167	0.875	0.840	
24.0	0.250	0.792	0.760	
34.0	0.333	0.708	0.680	
42.5	0.375	0.667	0.640	
54.0	0.417	0.625	0.600	
69.0	0.500	0.542	0.520	
82.0	0.542	0.500	0.480	
90.0	0.583	0.458	0.440	
104.0	0.625	0.417	0.400	
118.0	0.667	0.375	0.360	
232.0	0.708	0.333	0.320	
254.0	0.750	0.292	0.280	

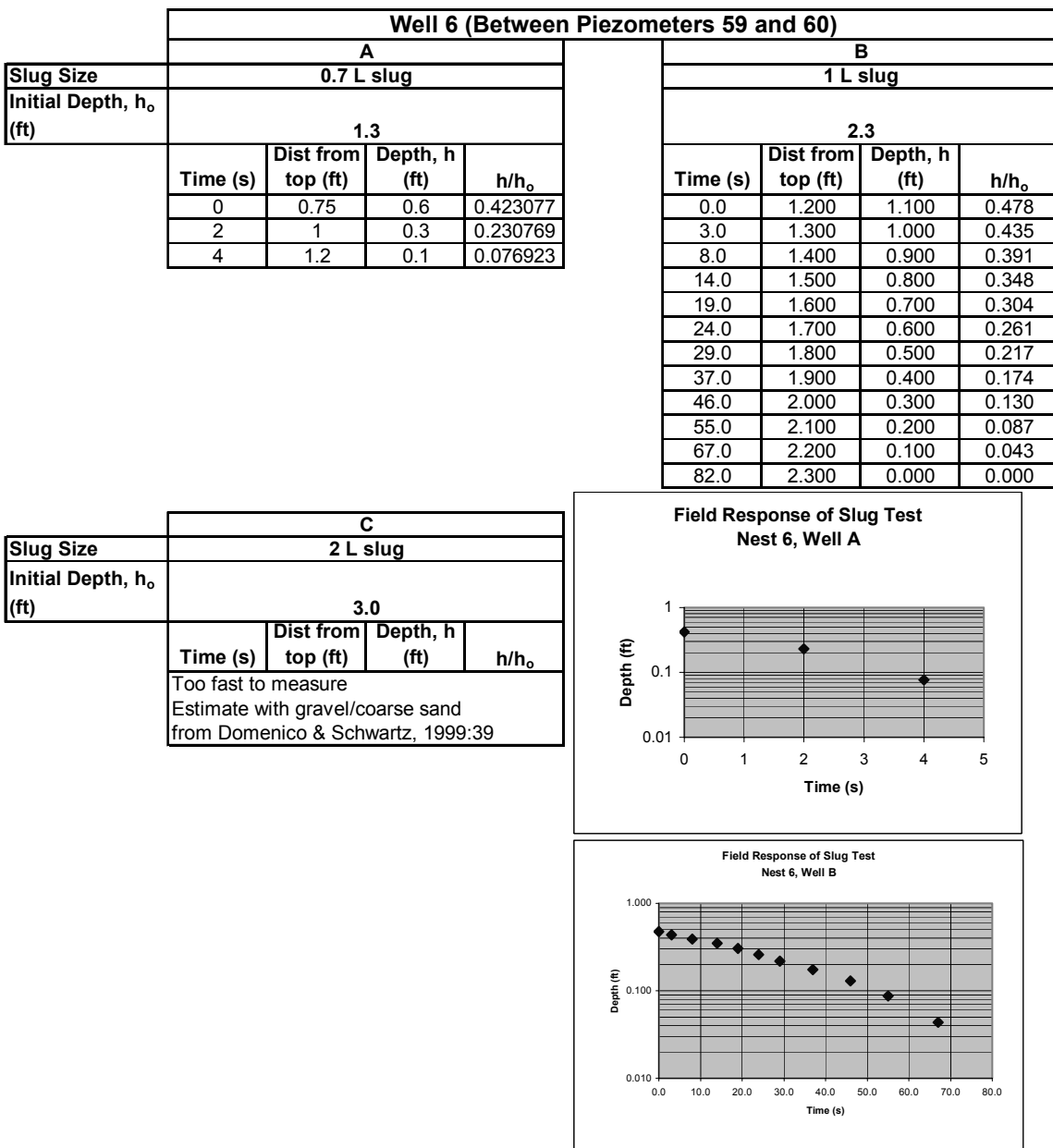
C				
Slug Size Initial Depth, h_o (ft)	2 L slug		3.40	
	3.40		3.40	
	Time (s)	Dist from top (ft)	Depth, h (ft)	h/h _o
0.0	1.000	2.400	0.706	
3.8	1.200	2.200	0.647	
6.0	1.300	2.100	0.618	
8.0	1.400	2.000	0.588	
10.0	1.500	1.900	0.559	
12.0	1.600	1.800	0.529	
15.0	1.700	1.700	0.500	
18.0	1.800	1.600	0.471	
21.0	1.900	1.500	0.441	
25.0	2.000	1.400	0.412	
29.0	2.100	1.300	0.382	
33.0	2.200	1.200	0.353	
38.0	2.300	1.100	0.324	
43.0	2.400	1.000	0.294	
49.5	2.500	0.900	0.265	
56.0	2.600	0.800	0.235	
65.0	2.700	0.700	0.206	
75.0	2.800	0.600	0.176	
88.0	2.900	0.500	0.147	
107.0	3.000	0.400	0.118	



Well 4 (Between Piezometers 39 and 40)					
Slug Size	A			B	
	0.7 L slug				
Initial Depth, h_o (ft)	1.20		3.85		No Data
	Time (s)	Dist from top (ft)	Depth, h (ft)	Time (s)	
	0.0	0.167	1.033	0.861	
	12.0	0.208	0.992	0.826	
	21.0	0.250	0.950	0.792	
	30.0	0.292	0.908	0.757	
	36.0	0.333	0.867	0.722	
	43.5	0.375	0.825	0.688	
	51.0	0.417	0.783	0.653	
	57.0	0.458	0.742	0.618	
	62.0	0.500	0.700	0.583	
	69.0	0.542	0.658	0.549	
	75.0	0.583	0.617	0.514	
	81.0	0.625	0.575	0.479	
	87.0	0.667	0.533	0.444	
	93.0	0.708	0.492	0.410	
	101.0	0.750	0.450	0.375	
	108.0	0.792	0.408	0.340	
	117.0	0.833	0.367	0.306	
	226.0	0.875	0.325	0.271	
C					
Slug Size	2 L slug			Field Response of Slug Test Nest 4, Well A	
Initial Depth, h_o (ft)	3.00				
	Time (s)	Dist from top (ft)	Depth, h (ft)	Time (s)	Depth (ft)
	0.0	1.5	1.500	0.0	1.000
	4.0	1.8	1.200	4.0	0.800
	6.5	2.2	0.800	10.0	0.600
	14.0	2.4	0.600	18.0	0.400
	18.0	2.5	0.500	25.0	0.300
	22.0	2.6	0.400	30.0	0.200
	25.0	2.7	0.300	34.0	0.100
	30.0	2.8	0.200	42.0	0.000
	34.0	2.9	0.100		
	42.0	3.0	0.000		
Field Response of Slug Test Nest 4, Well C					
	Time (s)	Depth (ft)	Time (s)	Depth (ft)	
	0.0	0.5	0.0	1.000	
	2.0	0.3	5.0	0.8	
	5.0	0.15	10.0	0.6	
	10.0	0.1	15.0	0.4	
	15.0	0.08	20.0	0.3	
	20.0	0.05	25.0	0.15	
	25.0	0.02	30.0	0.08	
	30.0	0.01	35.0	0.05	

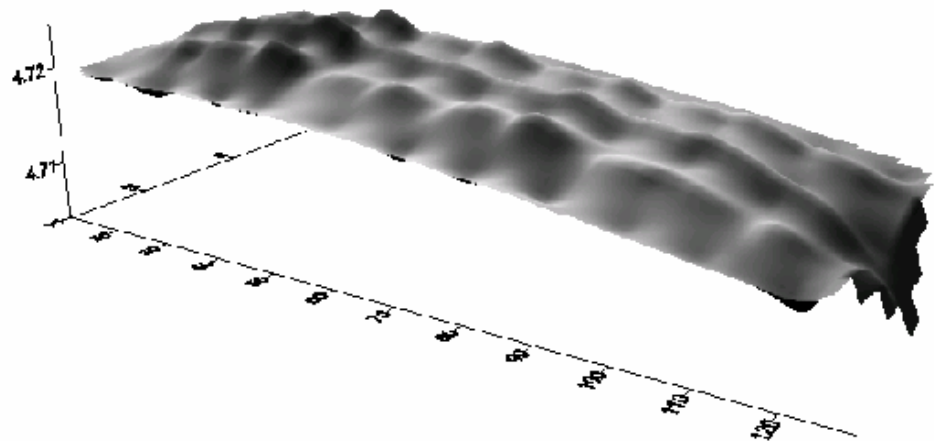
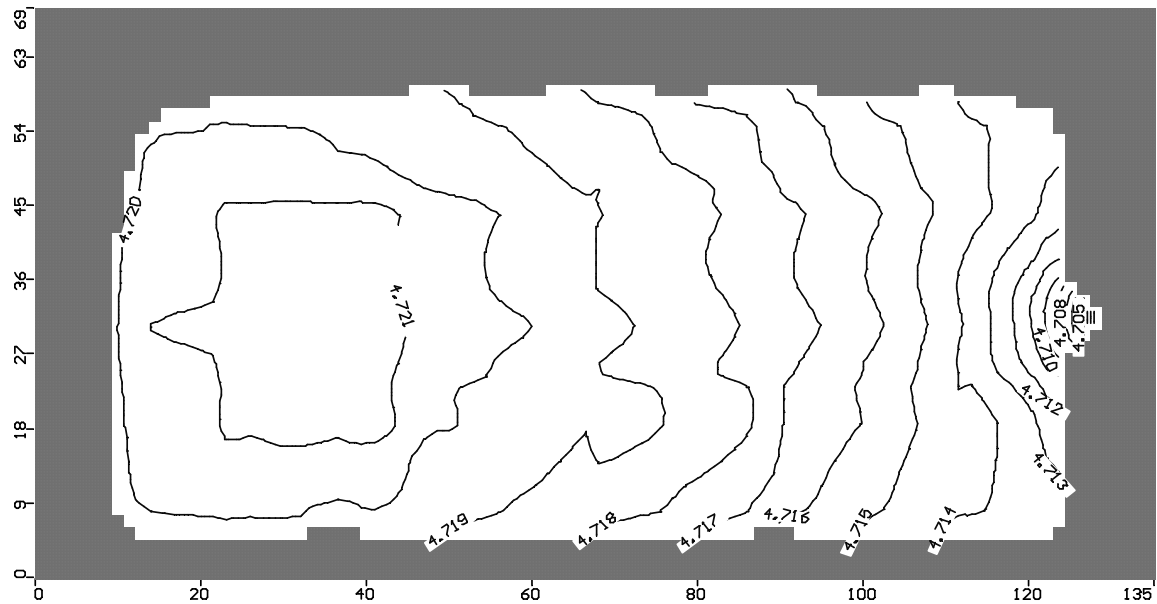
Well 5 (Between Piezometers 50 and 51)							
Slug Size	A			B			
	0.7 L slug						
Initial Depth, h_o (ft)							
		1.80					
Time (s)	Dist from top (ft)	Depth, h (ft)	h/h_o	Time (s)			
0.0	0.583	1.217	0.676	0.0	1.500	0.750	0.333
5.0	0.667	1.133	0.630	4.0	1.800	0.450	0.200
15.0	0.750	1.050	0.583	7.0	2.000	0.250	0.111
26.0	0.833	0.967	0.537	14.0	2.200	0.050	0.022
38.0	0.917	0.883	0.491	20.5	2.250	0.000	0.000
C							
Slug Size	1.7 L slug			Field Response of Slug Test Nest 5, Well A			
	2.60						
Time (s)	Dist from top (ft)	Depth, h (ft)	h/h_o	Depth (ft)	Time (s)		
0.0	0.292	2.308	0.888	0.100	0.0	0.800	
7.0	0.375	2.225	0.856	0.200	7.0	0.700	
11.0	0.417	2.183	0.840	0.300	11.0	0.650	
16.0	0.500	2.100	0.808	0.400	16.0	0.600	
21.0	0.542	2.058	0.792	0.500	21.0	0.550	
25.0	0.583	2.017	0.776	0.600	25.0	0.500	
29.0	0.625	1.975	0.760	0.700	29.0	0.450	
33.0	0.667	1.933	0.744	0.800	33.0	0.400	
36.5	0.708	1.892	0.728	0.900	36.5	0.350	
41.0	0.750	1.850	0.712	1.000	41.0	0.300	
45.0	0.792	1.808	0.696	1.100	45.0	0.250	
49.0	0.792	1.808	0.696	1.200	49.0	0.200	
59.0	0.833	1.767	0.679	1.300	59.0	0.150	
69.0	0.917	1.683	0.647	1.400	69.0	0.100	
80.0	1.100	1.500	0.577	1.500	80.0	0.050	
90.0	1.200	1.400	0.538	1.600	90.0	0.000	
111.0	1.300	1.300	0.500				
133.0	1.450	1.150	0.442				
140.0	1.500	1.100	0.423				
154.0	1.600	1.000	0.385				
172.0	1.700	0.900	0.346				
192.0	1.800	0.800	0.308				
213.0	1.900	0.700	0.269				
239.0	2.000	0.600	0.231				



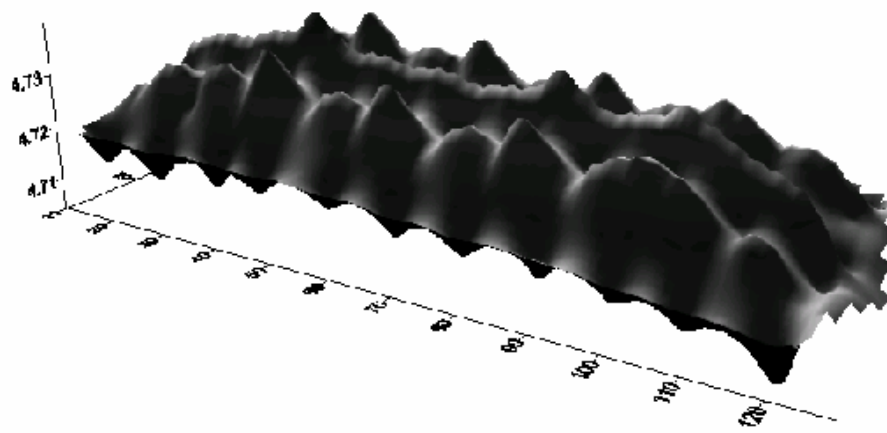
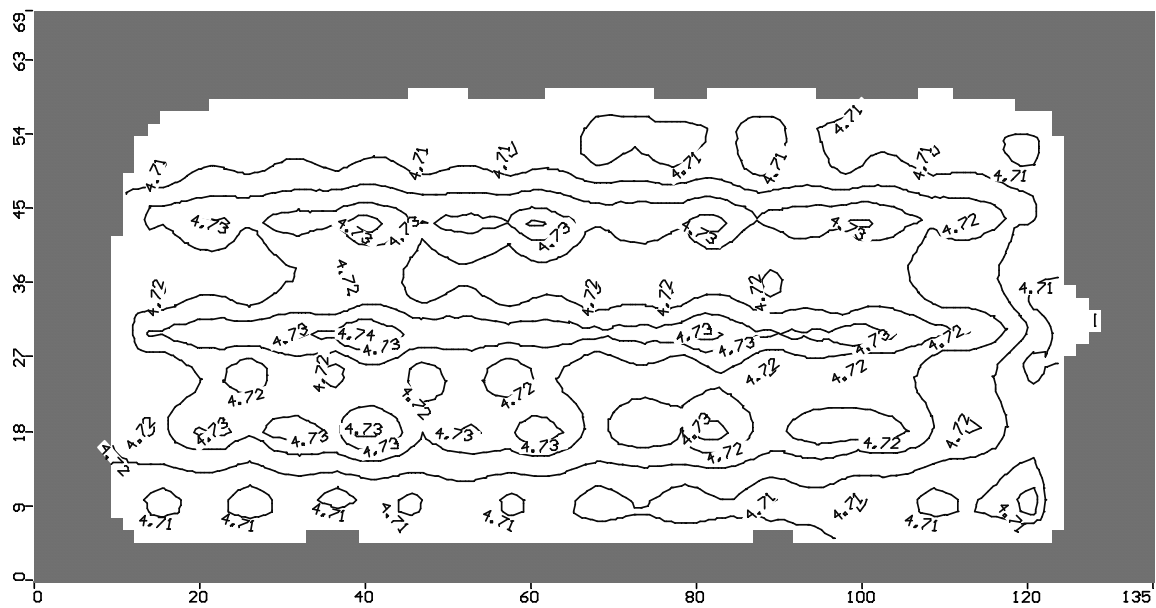


Appendix D: Equipotential Head Contour Plots

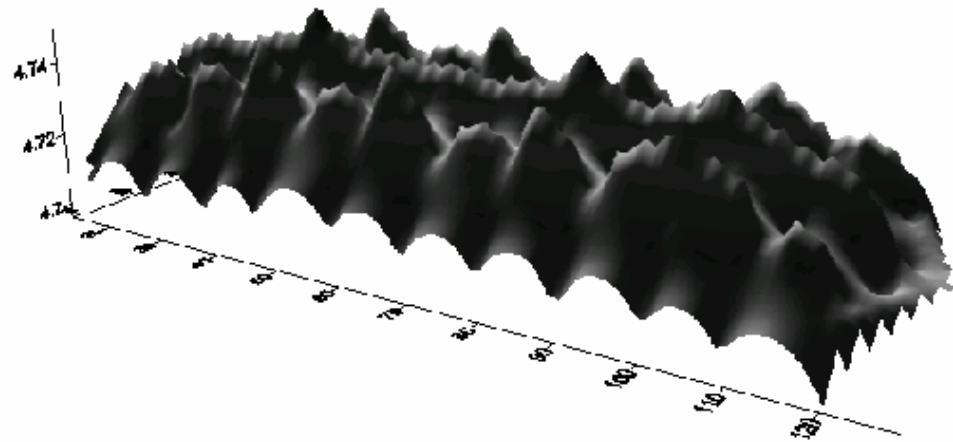
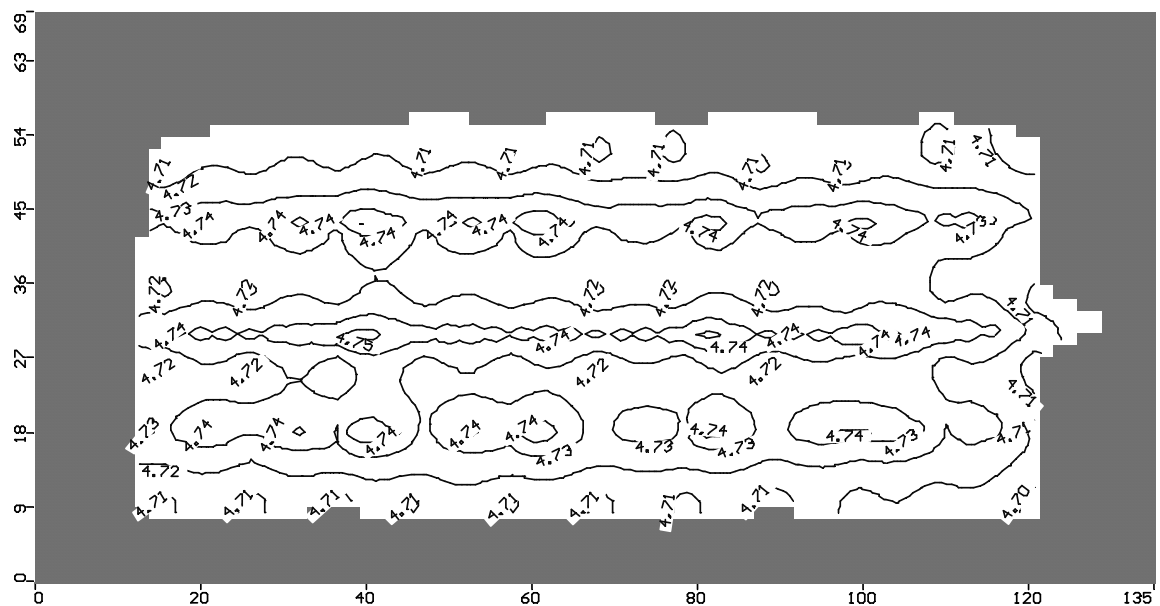
First Soil Layer



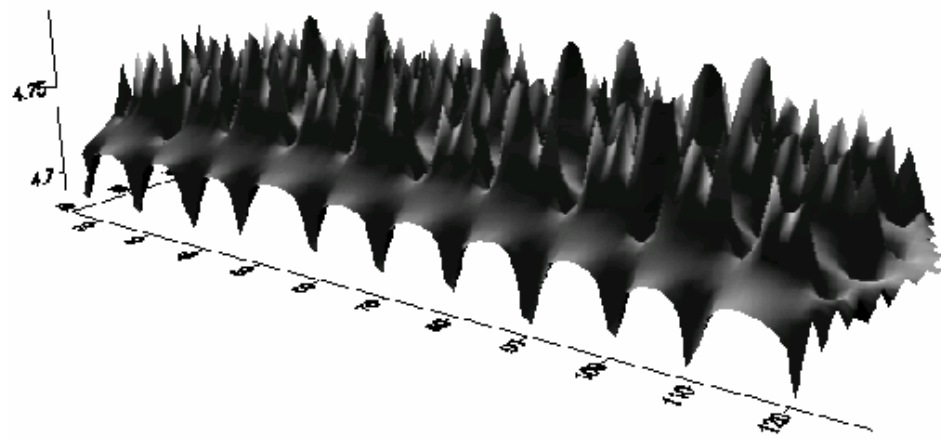
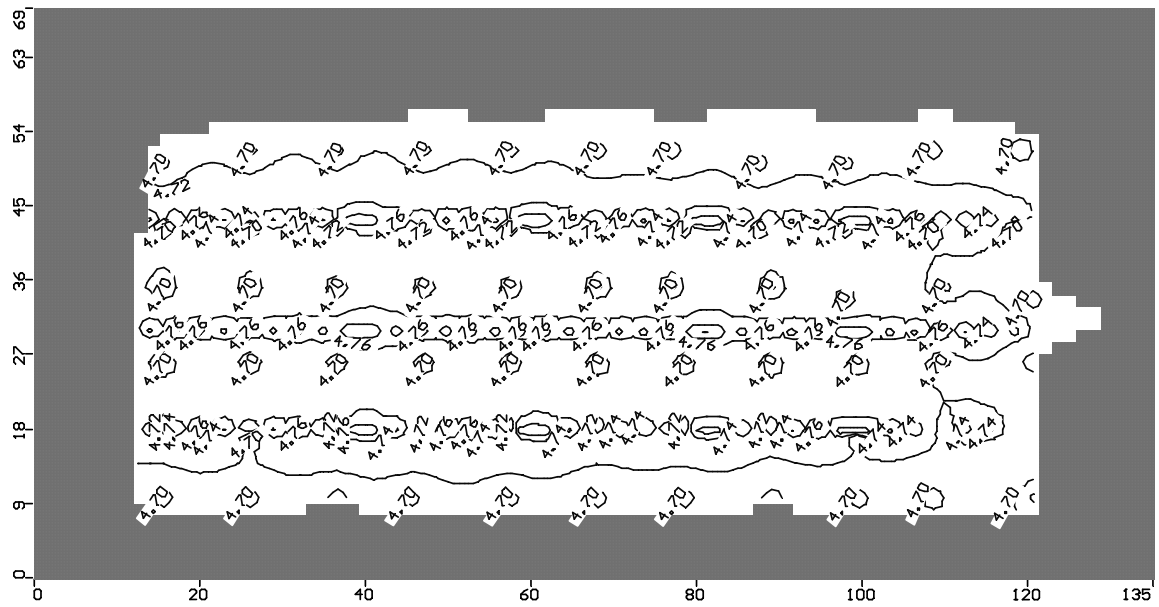
Second Soil Layer



Third Soil Layer

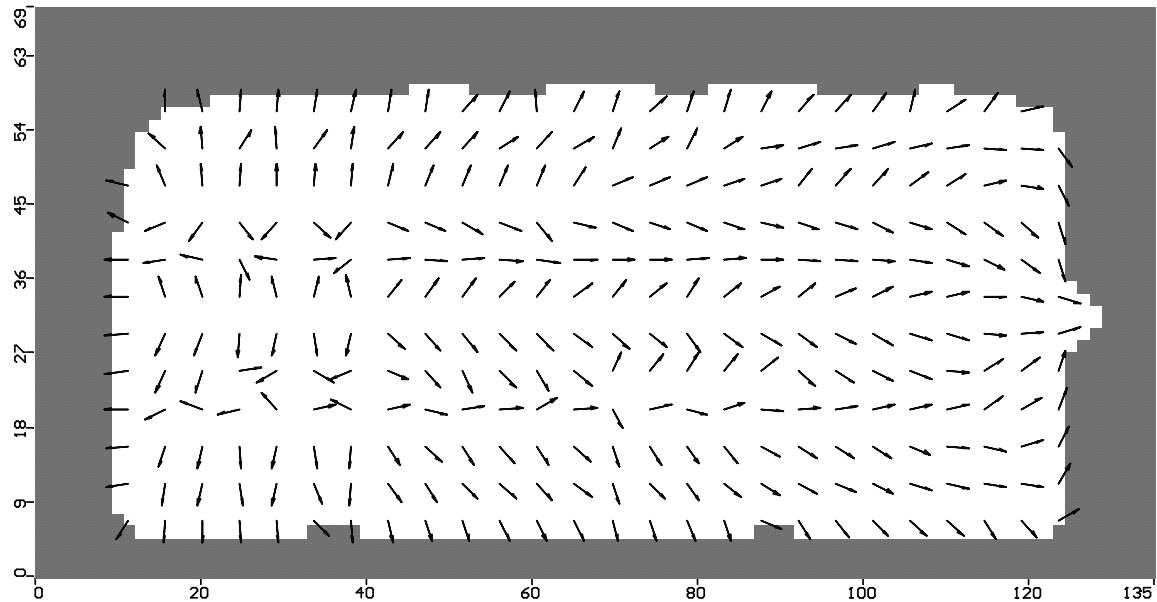


Gravel Layer

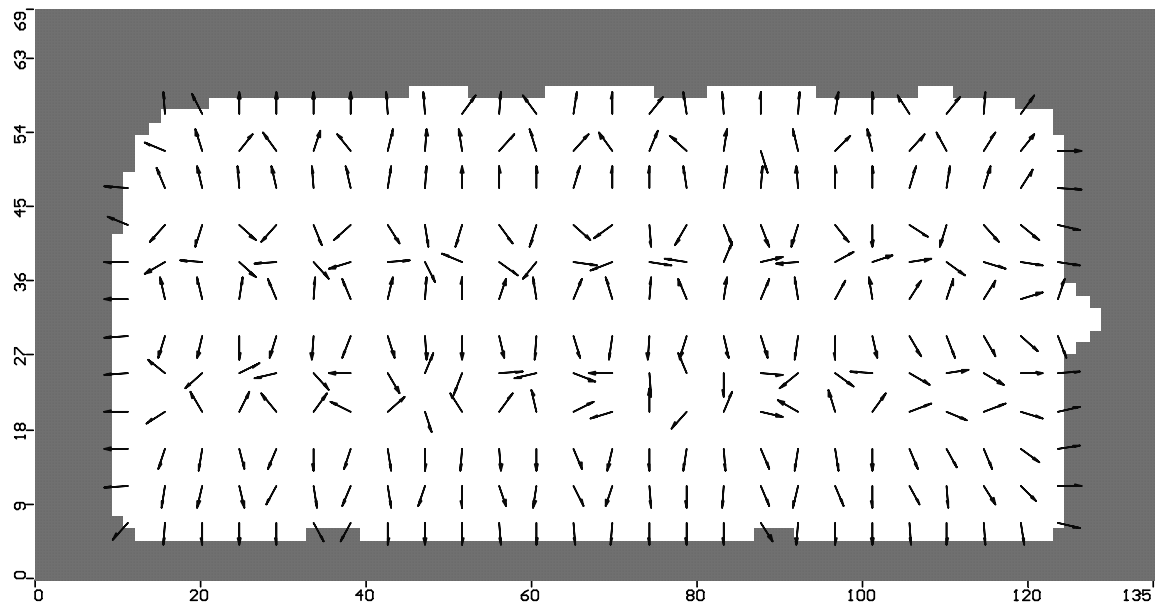


**Appendix E: Cross-Sections of the Wetland Model
Showing Flow Direction**

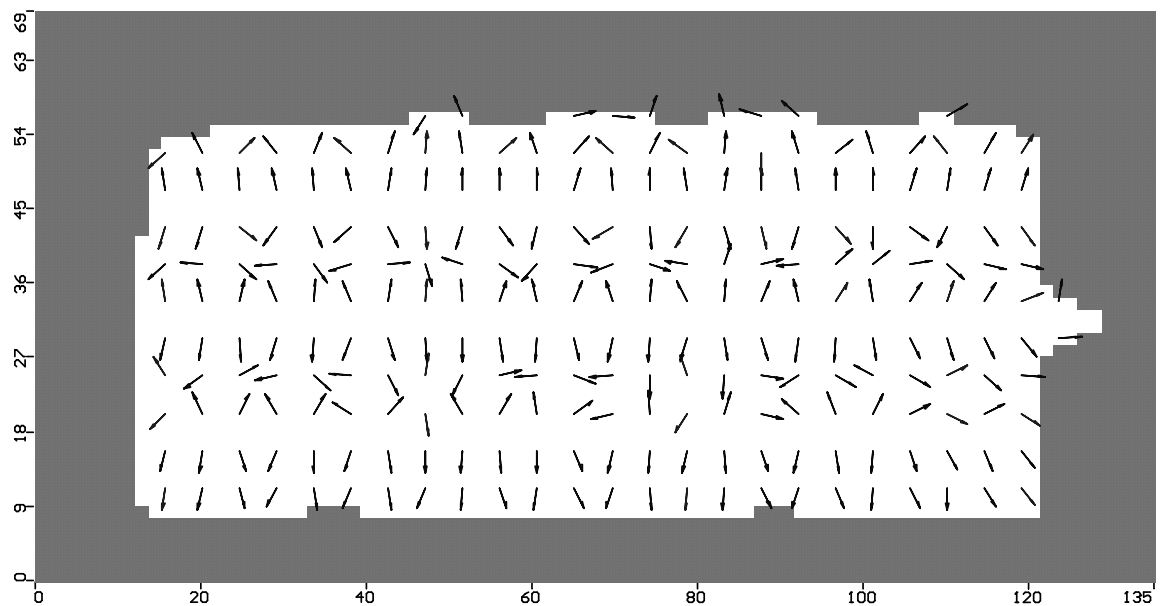
First Soil Layer



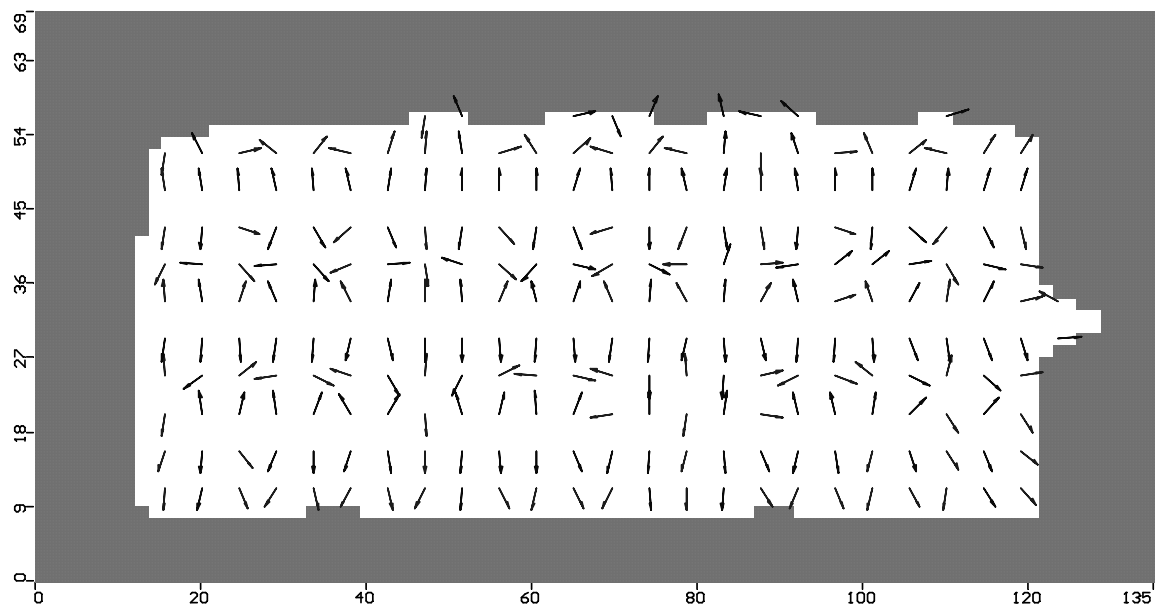
Second Soil Layer



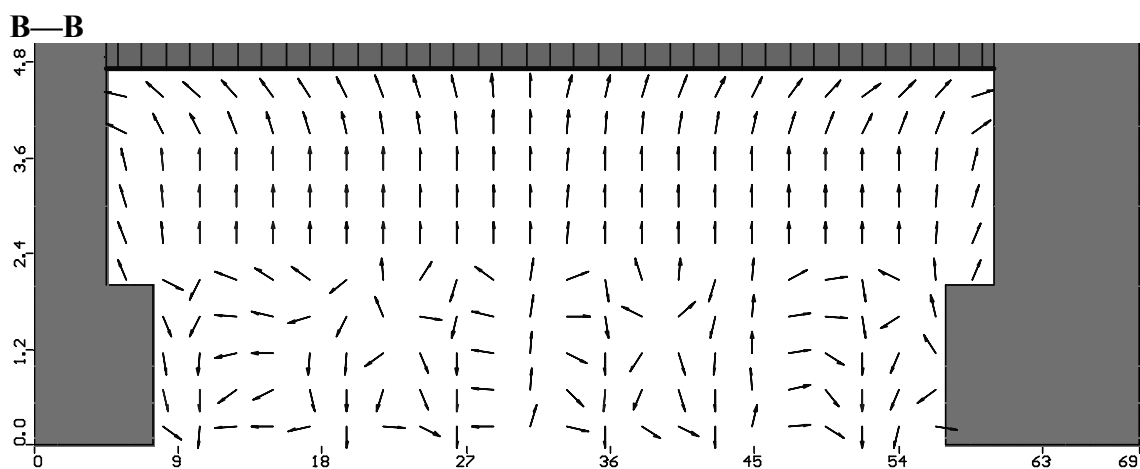
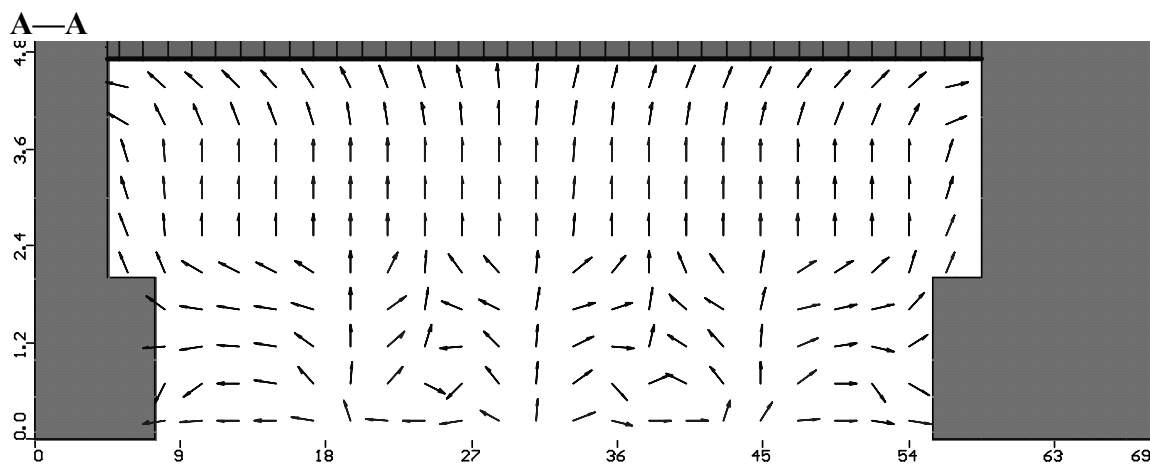
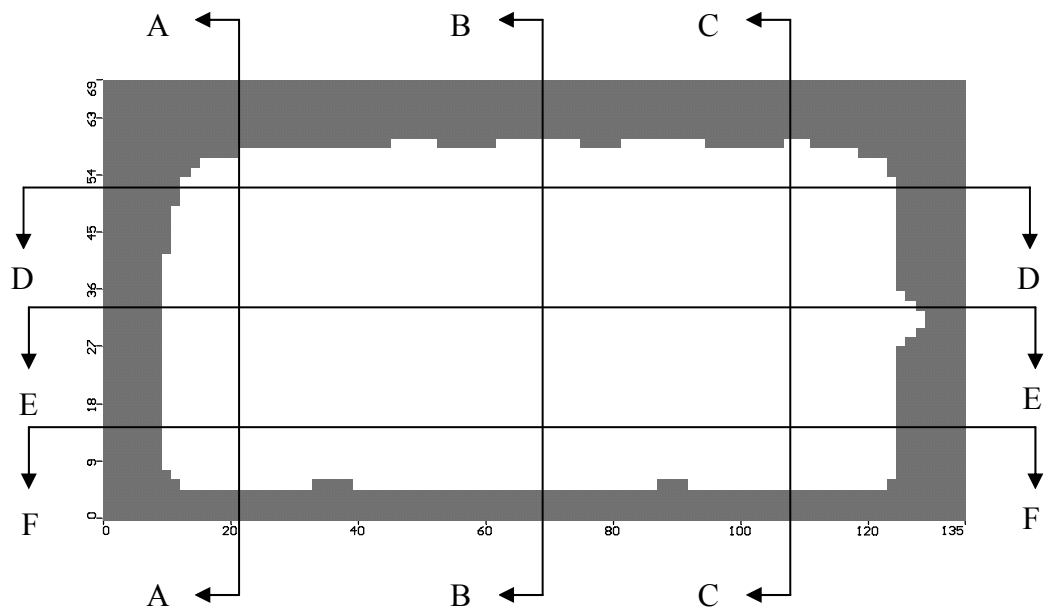
Third Soil Layer

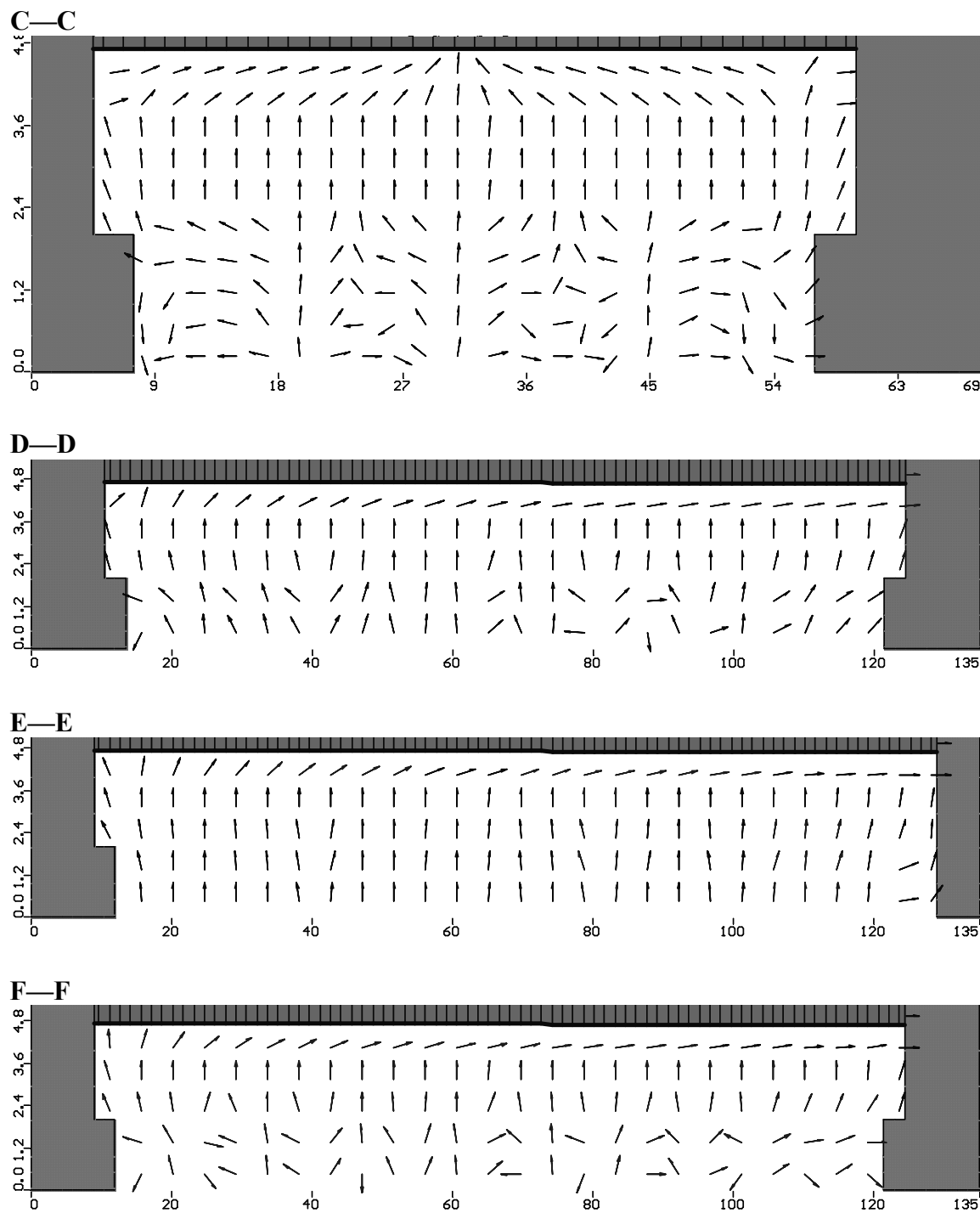


Gravel Layer



Elevation Views





Appendix F: Location Data of Particles through Wetland

A		
X	Y	Z
33.444	47.18	2.5
33.443	47.192	3
33.484	47.294	4
34.5	47.483	4.0579
36	47.75	4.1339
37.472	48	4.1991
37.5	48.005	4.2001
39	48.248	4.2515
40.5	48.48	4.2971
42	48.701	4.3379
43.5	48.913	4.3743
45	49.114	4.4071
46.5	49.305	4.4363
48	49.481	4.463
48.168	49.5	4.4658
49.5	49.644	4.4861
51	49.793	4.5071
52.5	49.932	4.5264
54	50.067	4.5442
55.5	50.202	4.5608
57	50.341	4.5763
58.5	50.485	4.5909
60	50.635	4.6046
61.5	50.79	4.6175
63	50.945	4.6297
63.552	51	4.6339
64.5	51.094	4.6409
66	51.229	4.6514
67.5	51.344	4.6618
69	51.437	4.6707
70.5	51.507	4.6794
72	51.558	4.6876
73.5	51.596	4.6953
75	51.631	4.7026
76.5	51.674	4.7095
78	51.732	4.716
79.5	51.805	4.7223
81	51.892	4.7284
82.5	51.986	4.7343
84	52.075	4.74
85.5	52.145	4.7455

B		
X	Y	Z
57.915	11.289	2.5
57.915	11.282	3
58.02	11.257	4
58.5	11.223	4.0113
60	11.12	4.0453
61.5	11.023	4.0772
63	10.93	4.1071
64.5	10.842	4.1354
66	10.759	4.1623
67.5	10.681	4.1896
69	10.609	4.2117
70.5	10.541	4.2339
71.504	10.5	4.2482
72	10.48	4.2548
73.5	10.424	4.2741
75	10.376	4.2926
76.5	10.337	4.3102
78	10.31	4.3271
79.5	10.296	4.3434
81	10.301	4.3589
82.5	10.328	4.3736
84	10.378	4.3876
85.5	10.444	4.4005
86.962	10.5	4.4118
87	10.501	4.4121
88.5	10.52	4.4238
89.714	10.5	4.4321
90	10.495	4.4337
91.5	10.429	4.4433
93	10.326	4.4533
94.5	10.222	4.4636
96	10.143	4.4737
97.5	10.099	4.4837
99	10.091	4.4934
100.5	10.117	4.5028
102	10.177	4.512
103.5	10.274	4.5209
105	10.411	4.5297
105.72	10.5	4.5337
106.5	10.595	4.5384
108	10.834	4.5472

87	52.188	4.7509
88.5	52.202	4.756
90	52.184	4.7606
91.5	52.137	4.7654
93	52.066	4.77
94.5	51.981	4.7743
96	51.892	4.7784
97.5	51.798	4.7823
99	51.696	4.7862
100.5	51.581	4.7899
102	51.444	4.7936
103.5	51.277	4.7971
105	51.069	4.8006
105.4	51	4.8013
106.5	50.812	4.8041
108	50.488	4.8076
109.5	50.074	4.8112
111	49.543	4.8147
111.1	49.5	4.8147
111.1	49.5	4.8147
112.5	48.899	4.8182
114	48.065	4.8219
114.1	48	4.8219
114.1	48	4.8219
115.5	47.042	4.8256
116.12	46.5	4.8271
117	45.732	4.8293
117.66	45	4.8308
118.5	44.06	4.8329
118.89	43.5	4.8337
119.94	42	4.8359
120	41.918	4.8355
120	41.918	4.8355
120.81	40.5	4.8366
121.5	39.341	4.837
121.64	39	4.8367
121.64	39	4.8367
122.37	37.5	4.836
123	36.485	4.8351
123.16	36	4.8344
124.5	34.653	4.8323
124.65	34.5	4.83
126	33.619	4.828
126.62	33	4.8246
127.5	32.65	4.8212
109.5	11.147	4.556
111	11.556	4.5649
112.24	12	4.5731
112.5	12.092	4.5748
114	12.776	4.5834
115.18	13.5	4.5909
115.5	13.7	4.5928
117	14.93	4.6029
117.07	15	4.6032
118.43	16.5	4.6128
118.5	16.582	4.6131
119.48	18	4.6199
120	18.795	4.6233
120.36	19.5	4.6253
121.11	21	4.6291
121.5	21.776	4.6305
121.77	22.5	4.6307
122.36	24	4.6307
122.36	24	4.6307
122.97	25.5	4.6305
123	25.55	4.6297
123.47	27	4.6293
124.5	28.033	4.6279
124.97	28.5	4.6263
126	29.175	4.625
126.82	30	4.6227
127.5	30.269	4.6202

C		
X	Y	Z
99.924	44.937	1.5
99.933	45	1.5396
100.13	46.5	1.6406
100.35	48	1.6535
100.5	48.951	1.6546
100.6	49.5	1.6552
100.92	51	1.6507
100.92	51	1.6507
101.35	52.5	1.6368
102	53.834	1.6017
102.12	54	1.5932
103.5	55.005	1.4514
105	55.326	1.1197
105.36	55.364	1
105.7	55.39	0.1
106.5	55.371	0.08155
108	55.138	0.053427
108.76	54	0.039973
109.05	52.5	0.033733

D		
X	Y	Z
89.729	19.242	1.5
90	19.405	1.8797
90.277	19.5	1.944
90.413	19.653	2
90.417	19.655	3
90.626	19.657	4
91.5	19.672	4.0151
93	19.705	4.0393
94.5	19.752	4.0621
96	19.816	4.0841
97.5	19.9	4.1052
99	20.01	4.1256
100.5	20.15	4.1451
102	20.325	4.1635
103.5	20.542	4.1808
105	20.807	4.1971
105.9	21	4.2063
106.5	21.123	4.2121
108	21.492	4.2258
109.5	21.932	4.2387
111	22.458	4.2511
111.1	22.5	4.2518
112.5	23.041	4.2629
114	23.726	4.2717
114.49	24	4.2744
115.5	24.487	4.2802
117	25.356	4.2881
117.2	25.5	4.2889
118.5	26.262	4.2942
119.52	27	4.2978
120	27.258	4.299
121.5	28.215	4.3023
121.86	28.5	4.3025
123	29.064	4.3039
124.5	29.796	4.3046
124.85	30	4.3039
124.85	30	4.3039
126	30.368	4.304
127.5	30.818	4.3029

E		
X	Y	Z
95.642	32.498	1.5
95.657	33	1.5482
95.733	34.5	1.5574
95.903	36	1.5406
95.903	36	1.5406
96	36.539	1.5273
96.238	37.5	1.4843
97.204	38.873	1
97.309	38.914	0.1
97.5	38.866	0.091402
99	38.454	0.030912
99.517	37.5	0.016061
99.63	36	0.009647
99	34.519	0.006898
98.997	34.5	0.006889

Appendix G: Residence Time Distribution Function Data

Time	# of Particles	F(t)	f(t)
0.95	0	0.0000	0.0000
1.00	0	0.0000	0.0000
1.05	1	0.0179	0.9219
1.10	6	0.1071	1.0360
1.15	7	0.1250	1.1092
1.20	12	0.2143	1.1474
1.25	19	0.3393	1.1560
1.30	20	0.3571	1.1398
1.35	22	0.3929	1.1033
1.40	23	0.4107	1.0506
1.45	25	0.4464	0.9855
1.50	30	0.5357	0.9114
1.55	32	0.5714	0.8312
1.60	34	0.6071	0.7476
1.65	36	0.6429	0.6630
1.70	38	0.6786	0.5794
1.75	41	0.7321	0.4987
1.80	41	0.7321	0.4222
1.85	43	0.7679	0.3512
1.90	43	0.7679	0.2866
1.95	43	0.7679	0.2293
2.00	45	0.8036	0.1796
2.05	45	0.8036	0.1379
2.10	45	0.8036	0.10431
2.00	45	0.8036	0.17960
2.05	45	0.8036	0.13791
2.10	45	0.8036	0.10431
2.15	45	0.8036	0.07874
2.20	45	0.8036	0.06095
2.25	45	0.8036	0.05057
2.30	46	0.8214	0.04707
2.35	46	0.8214	0.04981
2.40	46	0.8214	0.05804
2.45	47	0.8393	0.07092
2.50	47	0.8393	0.08753
2.55	47	0.8393	0.10688
2.60	47	0.8393	0.12795
2.65	47	0.8393	0.14965
2.70	47	0.8393	0.17091
2.75	48	0.8571	0.19062
2.80	49	0.8750	0.20770
2.85	50	0.8929	0.22107
2.90	51	0.9107	0.22970
2.95	52	0.9286	0.23262
3.00	53	0.9464	0.22890
3.05	53	0.9464	0.21771
3.10	53	0.9464	0.19831
3.15	53	0.9464	0.17005
3.2	54	0.9643	0.13243
3.45	55	0.9821	0.00000
4.25	56	1.0000	0.00000

Bibliography

Clark, Mark M. *Transport Modeling for Environmental Engineers and Scientists*. New York: John Wiley & Sons, 1996.

Dominico, Patrick A. and Schwartz, Franklin W. *Physical and Chemical Hydrogeology, (2nd Edition)*. New York: John Wiley & Sons, 1998.

Federal Register. Changes in Hydric Soils of the United States. Washington, DC. July 13, 1994.

Freeze, Allen R. and Cherry, John A. *Groundwater*. New Jersey: Prentice-Hall, Inc., 1979.

Gopal, Brij. Natural and Constructed Wetlands for Wastewater Treatment: Potential and Problems. *Water Science Technology*, 40: 27-35 (1999)

Hill, Mary. Water-Resources Investigations Report 90-4048. United States Geological Survey (1997)

Knight, Robert L. Wildlife Habitat and Public Use Benefits of Treatment Wetlands. *Water Science Technology*, 35: 35-43 (1997)

Knight, Robert L. and Kadlec, Robert H. Treatment Wetlands. Florida: Lewis Publishers, 1996.

Lorah, M.M. and L.D. Olsen. "Natural Attenuation of Chlorinated Volatile Organic Compounds in a Freshwater Tidal Wetland: Field Evidence of Anaerobic Biodegradation," *Water Resources Research*, 35(12): 3811-3827 (1999).

Masters, Gilbert M. *Introduction to Environmental Engineering and Science (2nd Edition)*. New Jersey: Prentice Hall, 1998.

Rash, Jonathan K. and Liehr, Sarah K. Flow Pattern Analysis of Constructed Wetlands Treating Landfill Leachate. *Water Science Technology*, 40: 309-315 (1999)

Reed, S.C., R.W. Crites, and E.J. Middlebrooks. Natural Systems for Waste Management and Treatment, 2nd Edition. New York: McGraw-Hill, Inc., 1995.

United States Environmental Protection Agency Office of Groundwater and Drinking Water: <http://www.epa.gov/safewater/sdwa/understand.pdf>

United States Environmental Protection Agency Office of Water: <http://www.epa.gov/owow/cwa/history.htm>

Vita

Captain Jack A. Blalock graduated from Helena High School in June 1993. He entered undergraduate studies at Montana State University in Bozeman, MT where he graduated with a Bachelor of Science degree in May 1998. He served in the Air Force Reserve Officer Training Corps (AFROTC) during college and was commissioned into the United States Air Force upon graduation.

As a commissioned officer, Captain Blalock served for two years as Energy Manager and Utility Engineer for the 92nd Civil Engineer Squadron at Fairchild Air Force Base, Spokane, WA. He then transferred jobs at the same base to Chief of Simplified Acquisition for Base Engineer Requirements for one year. In August 2001, Captain Blalock entered the Graduate School of Engineering and Management at the Air Force Institute of Technology. In October 2002 he passed the Environmental Professional Engineers exam. Following graduation, he will be assigned to the 341st Civil Engineer Squadron at Malmstrom Air Force Base, Great Falls, MT.

REPORT DOCUMENTATION PAGE				<i>Form Approved OMB No. 074-0188</i>
<p>The public reporting burden for this collection of information is estimated to average 1 hour per response, including the time for reviewing instructions, searching existing data sources, gathering and maintaining the data needed, and completing and reviewing the collection of information. Send comments regarding this burden estimate or any other aspect of the collection of information, including suggestions for reducing this burden to Department of Defense, Washington Headquarters Services, Directorate for Information Operations and Reports (0704-0188), 1215 Jefferson Davis Highway, Suite 1204, Arlington, VA 22202-4302. Respondents should be aware that notwithstanding any other provision of law, no person shall be subject to an penalty for failing to comply with a collection of information if it does not display a currently valid OMB control number.</p> <p>PLEASE DO NOT RETURN YOUR FORM TO THE ABOVE ADDRESS.</p>				
1. REPORT DATE (DD-MM-YYYY) 25-03-2003		2. REPORT TYPE Master's Thesis		3. DATES COVERED (From – To) Aug 2001 – Mar 2003
4. TITLE AND SUBTITLE GROUNDWATER FLOW THROUGH A CONSTRUCTED TREATMENT WETLAND			5a. CONTRACT NUMBER	
			5b. GRANT NUMBER	
			5c. PROGRAM ELEMENT NUMBER	
6. AUTHOR(S) Blalock, Jack A., USAF			5d. PROJECT NUMBER	
			5e. TASK NUMBER	
			5f. WORK UNIT NUMBER	
7. PERFORMING ORGANIZATION NAMES(S) AND ADDRESS(S) Air Force Institute of Technology Graduate School of Engineering and Management (AFIT/EN) 2950 P Street, Building 640 WPAFB OH 45433-7765				8. PERFORMING ORGANIZATION REPORT NUMBER AFIT/GEE/ENV/03-01
9. SPONSORING/MONITORING AGENCY NAME(S) AND ADDRESS(ES) AFRL/MLQ (AFMC) Dr. Tom Stauffer Barnes Avenue Tyndall AFB, FL 32403 (850)283-6859				10. SPONSOR/MONITOR'S ACRONYM(S) AFRL/MLQ
				11. SPONSOR/MONITOR'S REPORT NUMBER(S)
12. DISTRIBUTION/AVAILABILITY STATEMENT APPROVED FOR PUBLIC RELEASE; DISTRIBUTION UNLIMITED.				
13. SUPPLEMENTARY NOTES				
<p>14. ABSTRACT This study is an analysis of the flow of water through a constructed treatment wetland at Wright-Patterson AFB, OH. The purpose of the treatment wetland is to purify the groundwater contaminant perchloroethylene by microbial degradation. Contaminated water enters the bottom of the wetland and flows upward, then out a weir at one end. Efficient degradation takes place when the flow of water is as close to vertical as possible. The main purpose of this study is to characterize the flow paths chosen by water molecules through the varying layers of soil. Hydraulic parameters in the wetland are used to build a numerical model in Visual MODFLOW to help gather information about the residence time of the water molecules. Using the model, a Residence Time Distribution Function was developed to tell us how long water molecules are in the wetland, aiding in other studies for predicting the overall extent of reaction within the system. The mean residence time of water molecules that exited the weir was found to be 1.6 days. </p>				
<p>15. SUBJECT TERMS Groundwater Flow, Constructed Treatment Wetland, Upward Vertical Flow, Nested Piezometers </p>				
16. SECURITY CLASSIFICATION OF:		17. LIMITATION OF ABSTRACT UU	18. NUMBER OF PAGES 126	19a. NAME OF RESPONSIBLE PERSON Michael L. Shelley, PhD, Associate Professor, AFIT
a. REP ORT U	b. ABSTRA CT U	c. THIS PAGE U		19b. TELEPHONE NUMBER (Include area code) (937) 255-3636, ext 4594; e-mail: Michael.Shelley@afit.edu